

Studying the $b \rightarrow s\ell^+\ell^-$ Anomalies in RPV-MSSM Framework with Inverse Seesaw

Min-Di Zheng* and Hong-Hao Zhang†

School of Physics, Sun Yat-Sen University, Guangzhou 510275, China

Abstract

Inspired by the recent experimental results which show deviations from the standard model (SM) predictions of $b \rightarrow s\ell^+\ell^-$ transitions, we study the R -parity violating minimal supersymmetric standard model (RPV-MSSM) extended by the inverse seesaw mechanisms. The trilinear R -parity violating terms together with the chiral mixings of sneutrinos induce the loop contributions to the $b \rightarrow s\ell^+\ell^-$ anomaly. We study the parameter space of the single-parameter scenario $C_{9,\mu}^{\text{NP}} = -C_{10,\mu}^{\text{NP}} = C_V$, and the double-parameter scenario (C_V, C_U) respectively, constrained by other experimental data such as $B_s - \bar{B}_s$ mixing, $B \rightarrow X_s\gamma$ decay, the lepton flavour violating decays, etc.. Both the single-parameter scenario and double-parameter scenario can also resolve the long existed muon anomalous magnetic moment problem as well.

*zhengmd5@mail.sysu.edu.cn

†zhh98@mail.sysu.edu.cn

1 Introduction

In recent years, several hints of new physics (NP) beyond SM have shown up, such as, $R_{K^{(*)}} = \mathcal{B}(B \rightarrow K^{(*)}\mu^+\mu^-)/\mathcal{B}(B \rightarrow K^{(*)}e^+e^-)$ with the transition of $b \rightarrow s\ell^+\ell^-$ (where $\ell = e, \mu$) showing the very attracting anomalies. Especially, the measurement of R_K with the full run II data by the LHCb collaboration has just been updated as $R_K = 0.846^{+0.042}_{-0.039} {}^{+0.013}_{-0.012}$ in the q^2 bin $[1.1, 6] \text{ GeV}^2$ [1], which is much more precise than the previous one $R_K = 0.846^{+0.060}_{-0.054} {}^{+0.016}_{-0.014}$ [2], giving rise to the discrepancy with the SM value changing from preceding 2.5σ to 3.1σ . The recent measurements of R_{K^*} by LHCb give $R_{K^*} = 0.66^{+0.11}_{-0.07} \pm 0.03$ at $[0.045, 1.1] \text{ GeV}^2$ bin and $R_{K^*} = 0.69^{+0.11}_{-0.07} \pm 0.05$ at $[1.1, 6] \text{ GeV}^2$ bin, showing 2.1σ deviation at low q^2 region and 2.5σ one at high region, respectively [3]. The $R_{K^{(*)}}$ results by the Belle collaboration [4, 5] show the consistency with the SM predictions while having sizable experimental error bars. Besides, there are also other anomalies in the $b \rightarrow s\ell^+\ell^-$ transition. The angular observable P'_5 anomaly of $B \rightarrow K^*\mu^+\mu^-$ decay persists with the new data [6] compared with the run I results [7–12]. All these anomalies above show NP that breaks lepton flavour universality (LFU) may exist.

Ones know that each single anomaly above cannot be regarded as the conclusive evidence of NP. However, it is interesting that nearly all these anomalies can be explained simultaneously with the four-fermi operators in the model-independent global fit [13–25]. In light of the new measurement of R_K , there are already some new fit results updated [14, 21–25]. For the discussion of the global fit, the related Lagrangian of low energy effective field theory is given by here,

$$\mathcal{L}_{\text{eff}} = \frac{4G_F}{\sqrt{2}}\eta_t \sum_i C_i \mathcal{O}_i + \text{h.c.}, \quad (1.1)$$

where the CKM factor $\eta_t \equiv K_{tb}K_{ts}^*$. The main operators for the anomaly explanations are

$$\mathcal{O}_9 = \frac{e^2}{16\pi^2}(\bar{s}\gamma_\mu P_L b)(\bar{\ell}\gamma^\mu \ell), \quad \mathcal{O}_{10} = \frac{e^2}{16\pi^2}(\bar{s}\gamma_\mu P_L b)(\bar{\ell}\gamma^\mu \gamma_5 \ell), \quad (1.2)$$

where $P_L = (1 - \gamma_5)/2$ is the left-handed (LH) chirality projector and the Wilson coefficients $C_{9(10)} = C_{9(10)}^{\text{SM}} + C_{9(10)}^{\text{NP}}$. Among those abundant kinds of fit scenarios, there are two of them we will consider in this work and they can be given by an unified form,

$$\begin{aligned} C_{9,\mu}^{\text{NP}} &= C_V + C_U, & C_{10,\mu}^{\text{NP}} &= -C_V, \\ C_{9,e}^{\text{NP}} &= C_U, & C_{10,e}^{\text{NP}} &= 0, \end{aligned} \quad (1.3)$$

where V denotes the contributions only of $\mu^+\mu^-$ channel and U denotes LFU contributions. The first scenario, named scenario A here, requires $C_U = 0$ so it is the single-parameter-scenario $C_{9,\mu}^{\text{NP}} = -C_{10,\mu}^{\text{NP}}$ in fact. We adopt the fit result $-0.5 < C_V < -0.36$ to conform to all the rare B -meson decays at 1σ level in Ref. [22]. Except the new R_K measurement [1], authors in Ref. [22] have also considered series of new experimental results, such as the new angular analyses of $B^0 \rightarrow K^{*0}\mu^+\mu^-$ [6] and $B^\pm \rightarrow K^{*\pm}\mu^+\mu^-$ [26] as well as the last results of $B \rightarrow \mu^+\mu^-$ from CMS [27] and LHCb [28]. Correspondingly, for the scenario B demanding $C_U \neq 0$, we also adopt the fit regions in Ref. [22] with the best fit point $(C_V, C_U) \approx (-0.34, -0.50)$.

After these results of model-independent analyses gotten, imperative works are remained to find the concrete NP models which can conform to them. Ones know that both the scenario A and B have been implemented in RPV-MSSM [29–34]. The crucial difference of the two scenarios is whether the logarithmic enhancement of LH sneutrinos in photonic penguins exists [33]. When masses of LH sneutrinos are sufficient heavy or there is a cancelling out in the penguin contribution [32], the scenario B turns into the scenario A.

More than RPV-MSSM, the inverse seesaw mechanism within supersymmetric (SUSY) [35] or two-Higgs doublet frameworks [36] is also researched for the explanation of $b \rightarrow s\ell^+\ell^-$ disparities. The seesaw mechanism [37–43] is one of the most noted methods to generate neutrino masses and is thought as the most natural, given that the conclusive evidence of neutrino oscillations [44]. As one type of seesaw mechanisms, the inverse seesaw [45, 46] can give a $\mathcal{O}(1)$ neutrino Yukawa coupling Y_ν [47, 48]. It was found that the lightest right-handed (RH) sneutrinos engaged with charginos in the box diagram can singly explain $R_{K^{(*)}}$ discrepancies ever [35]. The relative large Y_ν implicates that the admixture between LH neutrino superfields and RH or extra singlet ones is not negligible. So it will be meaningful to study the chiral mixings of (s)neutrinos in MSSM framework including both inverse seesaw mechanisms and the tree level trilinear RPV terms, then all chiral parts of (s)neutrinos can interact with (s)quarks. This new combination is naturally reasonable [49] and has never be studied in the $b \rightarrow s\ell^+\ell^-$ anomalies to our knowledge.

The recent combined results [50] of $R(D^{(*)}) = \mathcal{B}(B \rightarrow D^{(*)}\tau\nu)/\mathcal{B}(B \rightarrow D^{(*)}\ell\nu)$ in charged current $b \rightarrow c\tau\nu$ from the measurements of BaBar [51, 52], Belle [53–56] and LHCb [57–59] also show the tension with SM [60–63]. While the new results of $R(D^{(*)})$ from Belle using the semileptonic tagging method, such as the most newly updated one with the data sample of $772 \times 10^6 B\bar{B}$ pairs, are already in agreement with SM predictions well. Belle combined results

are consistent with SM predictions within 1.6σ [64]. Given this, we just do not investigate $R(D^{(*)})$ in this work.

The clues of LFU violation exist not only in B -meson decay processes, but also in other transitions, such as, the muon anomalous magnetic moment problem which has existed several decades. The measurement of $a_\mu = (g - 2)_\mu$ by Fermilab [65–67] just presents 3.3σ deviations greater than the SM prediction [68]¹, and agrees with the previous Brookhaven E821 experiment [74]. The combined average of the two experiments, $\Delta a_\mu = a_\mu^{\text{exp}} - a_\mu^{\text{SM}} = (2.51 \pm 0.59) \times 10^{-9}$ shows the increased tension at the significant 4.2σ level and it is a growing motivation of NP. For electron anomalous magnetic moment, there is a negative 2.4σ discrepancy between the measurement [75] and the SM prediction [76], $\Delta a_e = a_e^{\text{exp}} - a_e^{\text{SM}} = (-8.7 \pm 3.6) \times 10^{-13}$, due to the new measurement of the fine structure constant in Ref. [77]². There are plentiful articles discussing the $(g - 2)_\mu$ problem in the SUSY framework, including but not limited to recent Refs. [34, 48, 80–109]. In this work, we will investigate whether the parameter space for the explanation of $b \rightarrow s\ell^+\ell^-$ anomalies can accord with the deviations between the measurement of a_μ and its SM prediction, and then we discuss the NP effects on a_e .

Our paper is organized as follows. The new model in this work is introduced firstly in section 2. Then in section 3, the whole one-loop contributions in this model to the $b \rightarrow s\ell^+\ell^-$ transition are scrutinized and we emphasize the main contributions to explain the $b \rightarrow s\ell^+\ell^-$ anomaly in our parameter scheme. We discuss NP contributions to $(g - 2)_\ell$ and other related constraints in section 4 followed by the numerical analyses in section 5. Our conclusions are finally made in section 6.

2 The Model

The model considered in this work is R -parity violating MSSM with inverse seesaw mechanisms (RPV-MSSMIS) and the superpotential is expressed by,

$$\mathcal{W} = \mathcal{W}_{\text{MSSM}} + Y_\nu^{ij} \hat{R}_i \hat{L}_j \hat{H}_u + M_R^{ij} \hat{R}_i \hat{S}_j + \frac{1}{2} \mu_S^{ij} \hat{S}_i \hat{S}_j + \lambda'_{ijk} \hat{L}_i \hat{Q}_j \hat{D}_k, \quad (2.1)$$

¹One recent calculation of the hadronic vacuum polarization [69] weakens the discrepancy between the experiment and SM prediction of a_μ while it shows the tension with the R-ratio determinations [70–73]. We have not considered this result here but the preceding review of various SM results [68].

²It should be mentioned another new measurement of the fine structure constant [78] differs by more than 5σ to the previous one [77] and affects the deviation Δa_e to positive 1.6σ level [79]. The NP hint searching in a_e still expects more experimental researches and we focus on a_μ anomaly explanations in this work while discuss the effects on a_e in our model.

where the generation indices $i, j, k = 1, 2, 3$ while the colour ones are suppressed, and from here on, all the repeated indices are defaulted to be summed over unless otherwise stated. Here the superpotential of MSSM [110, 111] is expressed as,

$$\mathcal{W}_{\text{MSSM}} = \mu \hat{H}_u \hat{H}_d + Y_u^{ij} \hat{U}_i \hat{Q}_j \hat{H}_u - Y_d^{ij} \hat{D}_i \hat{Q}_j \hat{H}_d - Y_e^{ij} \hat{E}_i \hat{L}_j \hat{H}_d. \quad (2.2)$$

In RPV-MSSMIS, MSSM superfields are extended by three generations of pairs of SM singlet superfields, \hat{R}_i and \hat{S}_i . The neutral parts of two Higgs doublet superfields $\hat{H}_u = (\hat{H}_u^+, \hat{H}_u^0)^T$ and $\hat{H}_d = (\hat{H}_d^0, \hat{H}_d^-)^T$ acquire the non-zero vacuum expectation value, $\langle \hat{H}_u^0 \rangle = v_u$ and $\langle \hat{H}_d^0 \rangle = v_d$ respectively, leading to the mixing angle $\beta = \tan^{-1}(v_u/v_d)$. The tree level trilinear RPV coupling $\lambda'_{ijk} \hat{L}_i \hat{Q}_j \hat{D}_k$ can be added for \hat{L}_i sharing the same SM quantum number with \hat{H}_d . It is needed to point out that the RPV superpotential terms like $\lambda'_{ijk} \hat{L}_i \hat{Q}_j \hat{D}_k$, $\lambda_{ijk} L_i L_j E_k$, $\lambda''_{ijk} U_i D_j D_k$ as well as $\mu_i \hat{L}_i \hat{H}_u$ are all in principle allowed for SM gauge invariance if there is no extra model symmetries. Here we only consider the term $\lambda'_{ijk} \hat{L}_i \hat{Q}_j \hat{D}_k$ relating the quark sector to lepton sector without the term $\lambda''_{ijk} U_i D_j D_k$ within pure quark sectors or the purely lepton interaction $\lambda_{ijk} L_i L_j E_k$, because of the attempt to avoid the disastrously rapid proton decay when there are nonzero parameters λ' and λ'' simultaneously and the strong collider constraints on the lightest sneutrino mass when the λ' and λ both exist [112–115]. We also take no account of the bilinear term $\mu_i \hat{L}_i \hat{H}_u$, which can make some contributions to neutrino masses [116], and we do not need this term when already having seesaw terms to generate neutrino masses just at tree level. With the scalar components of Higgs doublet superfields denoted by H_u and H_d , and squarks and sleptons denoted by “ $\tilde{}$ ”, the soft supersymmetry breaking Lagrangian is given by,

$$\begin{aligned} -\mathcal{L}^{\text{soft}} = & -\mathcal{L}_{\text{MSSM}}^{\text{soft}} + (m_{\tilde{R}}^2)_{ij} \tilde{R}_i^* \tilde{R}_j + (m_{\tilde{S}}^2)_{ij} \tilde{S}_i^* \tilde{S}_j \\ & + (A_\nu Y_\nu)_{ij} \tilde{R}_i^* \tilde{L}_j H_u + B_{M_R}^{ij} \tilde{R}_i^* \tilde{S}_j + \frac{1}{2} B_{\mu_S}^{ij} \tilde{S}_i \tilde{S}_j, \end{aligned} \quad (2.3)$$

where $\mathcal{L}_{\text{MSSM}}^{\text{soft}}$ corresponds to MSSM part [110, 111]. It should be mentioned that MSSM and singlet neutrino sectors are all at low scale (around 1 TeV) in this work, so some terms in the most general superpotential and soft breaking Lagrangian are already or will be vanished ad hoc for the phenomenology consideration.

As to the three terms following $\mathcal{W}_{\text{MSSM}}$ in Eq. (2.1) which give the neutrino mass spectrum

at tree level, the 9×9 mass matrix of neutrino in the (ν_i, R_i, S_i) basis is given by,

$$\mathcal{M}_\nu = \begin{pmatrix} 0 & m_D^T & 0 \\ m_D & 0 & M_R \\ 0 & M_R^T & \mu_S \end{pmatrix}, \quad (2.4)$$

in which $m_D = \frac{1}{\sqrt{2}}v_u Y_\nu^T$. And the μ_S parameter can be gotten by,

$$\mu_S = (m_D^T)^{-1} M_R U_{\text{PMNS}} m_\nu^{\text{diag}} U_{\text{PMNS}}^T M_R^T m_D^{-1}, \quad (2.5)$$

when $\mu_S \ll m_D < M_R$. The neutrino mass $\mathcal{M}_\nu^{\text{diag}}$ in physics basis containing the three-light-generation part m_ν^{diag} in Eq. (2.5), is given by $\mathcal{M}_\nu^{\text{diag}} = \mathcal{V} \mathcal{M}_\nu \mathcal{V}^T$. Here embedded in the whole 9×9 mixing matrix \mathcal{V}^T , the 3×3 light-generation sector $\mathcal{V}_{3 \times 3}^T$ should approximate the PMNS matrix U^{PMNS} [44, 117].

Then we turn to the sneutrino mass square matrix in the $(\tilde{\nu}_L^{\mathcal{I}(\mathcal{R})}, \tilde{R}^{\mathcal{I}(\mathcal{R})}, \tilde{S}^{\mathcal{I}(\mathcal{R})})$ basis, which is expressed as,

$$\mathcal{M}_{\tilde{\nu}^{\mathcal{I}(\mathcal{R})}}^2 = \begin{pmatrix} m_{\tilde{L}'}^2 & (A_\nu - \mu \cot \beta) m_D^T & m_D^T M_R \\ (A_\nu - \mu \cot \beta) m_D & m_{\tilde{R}}^2 + (M_R M_R^T) + (m_D m_D^T) & \pm M_R \mu_S + B_{M_R} \\ M_R^T m_D & \pm \mu_S M_R^T + B_{M_R}^T & m_{\tilde{S}}^2 + \mu_S^2 + M_R^T M_R \pm B_{\mu_S} \end{pmatrix}, \quad (2.6)$$

where the “ \pm ” above expresses the CP-even and CP-odd, and also CP-odd is denoted by \mathcal{I} and CP-even is denoted by \mathcal{R} . The soft mass $m_{\tilde{L}'}^2 = m_{\tilde{L}}^2 + \frac{1}{2} m_Z^2 \cos 2\beta + (m_D^T m_D)$ can be regarded as one whole input where $m_{\tilde{L}}^2$ is the soft mass square of \tilde{L} in $\mathcal{L}_{\text{MSSM}}^{\text{soft}}$. It should be paid attention to that the CP-even and CP-odd masses can be nearly the same for tiny μ_S and relative small B_{μ_S} [118]. Besides, the value of $m_{\tilde{S}}^2$ is set to be zero here. Thus, ones have [119]

$$\mathcal{M}_{\tilde{\nu}^{\mathcal{I}(\mathcal{R})}}^2 \approx \begin{pmatrix} m_{\tilde{L}'}^2 & (A_\nu - \mu \cot \beta) m_D^T & m_D^T M_R \\ (A_\nu - \mu \cot \beta) m_D & m_{\tilde{R}}^2 + (M_R M_R^T) + (m_D m_D^T) & B_{M_R} \\ M_R^T m_D & B_{M_R}^T & M_R^T M_R \end{pmatrix}. \quad (2.7)$$

In the following we adopt this particular structure and then the mixing matrices $\tilde{\mathcal{V}}^{\mathcal{I}(\mathcal{R})}$, which diagonalize sneutrino mass square matrices by $\tilde{\mathcal{V}}^{\mathcal{I}(\mathcal{R})} \mathcal{M}_{\tilde{\nu}^{\mathcal{I}(\mathcal{R})}}^2 \tilde{\mathcal{V}}^{\mathcal{I}(\mathcal{R})\dagger} = (\mathcal{M}_{\tilde{\nu}^{\mathcal{I}(\mathcal{R})}}^2)^{\text{diag}}$, are also the

same whether CP even or odd. Thus all the $\tilde{\mathcal{V}}^{\mathcal{R}}$ and the physics mass $m_{\tilde{\nu}_v^{\mathcal{R}}}$ can be expressed as $\tilde{\mathcal{V}}^{\mathcal{I}}$ and $m_{\tilde{\nu}_v^{\mathcal{I}}}$, respectively in the rest of the paper. With respect to charged sleptons, the LH sector element will be expressed by $m_{\tilde{L}}^2 + m_l^2 - m_D^T m_D - m_Z^2 \cos^2 \theta_W \cos 2\beta$.

Afterwards we illustrate the last term of the superpotential. For the superpotential term $\lambda'_{ijk} \hat{L}_i \hat{Q}_j \hat{D}_k$, the corresponding Lagrangian in the flavour basis is obtained as,

$$\begin{aligned} \mathcal{L}_{\text{LQD}} = & \lambda'_{ijk} (\tilde{\nu}_{Li} \bar{d}_{Rk} d_{Lj} + \tilde{d}_{Lj} \bar{d}_{Rk} \nu_{Li} + \tilde{d}_{Rk}^* \bar{\nu}_{Li}^c d_{Lj} \\ & - \tilde{l}_{Li} \bar{d}_{Rk} u_{Lj} - \tilde{u}_{Lj} \bar{d}_{Rk} l_{Li} - \tilde{d}_{Rk}^* \bar{l}_{Li}^c u_{Lj}) + \text{h.c.}, \end{aligned} \quad (2.8)$$

where “ c ” indicates the charge conjugated fermions. Then in the context of mass eigenstates for the down quarks and charged leptons, the Lagrangian above with other fields $\tilde{\nu}_L$, ν_L and u_L aligned with \tilde{u}_L rotated to mass eigenstates by mixing matrices $\tilde{\mathcal{V}}^{\mathcal{I}(\mathcal{R})}$, \mathcal{V} and K respectively, is given by,

$$\begin{aligned} \mathcal{L}'_{\text{LQD}} = & \lambda_{vjk}^{\mathcal{I}(\mathcal{R})} \tilde{\nu}_v \bar{d}_{Rk} d_{Lj} + \lambda_{vjk}^{\mathcal{N}} (\tilde{d}_{Lj} \bar{d}_{Rk} \nu_v + \tilde{d}_{Rk}^* \bar{\nu}_v^c d_{Lj}) \\ & - \tilde{\lambda}'_{ilk} (\tilde{l}_{Li} \bar{d}_{Rk} u_{Ll} + \tilde{u}_{Ll} \bar{d}_{Rk} l_{Li} + \tilde{d}_{Rk}^* \bar{l}_{Li}^c u_{Ll}) + \text{h.c.}, \end{aligned} \quad (2.9)$$

then all the fields are in the mass eigenstates. Concretely, ν_v and $\tilde{\nu}_v$ are in the mass eigenstate with the index $v = 1, 2, \dots, 9$ and the three neo- λ' terms are deduced as $\lambda_{vjk}^{\mathcal{I}(\mathcal{R})} = \lambda'_{ijk} \tilde{\mathcal{V}}_{vi}^{\mathcal{I}(\mathcal{R})*}$, $\lambda_{vjk}^{\mathcal{N}} = \lambda'_{ijk} \mathcal{V}_{vi}^*$ and $\tilde{\lambda}'_{ilk} = \lambda'_{ijk} K_{lj}^*$. In the following, we call the diagrams including these λ' couplings by “ λ' diagrams”, otherwise by “non- λ' diagrams”.

By the end of this section, we should mention the chargino and neutralino mass matrix in the MSSM sector of this model. The chargino mass matrix is,

$$\mathcal{M}_{\chi^\pm} = \begin{pmatrix} M_2 & \sqrt{2} m_w \sin \beta \\ \sqrt{2} m_w \cos \beta & \mu \end{pmatrix}, \quad (2.10)$$

where the parameter M_2 is related to wino mass and μ is related to Higgsino mass. The mixing matrix V and U diagonalize \mathcal{M}_{χ^\pm} by $U^* \mathcal{M}_{\chi^\pm} V^\dagger = \mathcal{M}_{\chi^\pm}^{\text{diag}}$. As to the neutralino mass matrix

\mathcal{M}_{χ^0} in the basis $(\tilde{B}, \tilde{W}^3, \tilde{H}_d^0, \tilde{H}_u^0)^T$,

$$\mathcal{M}_{\chi^0} = \begin{pmatrix} M_1 & 0 & -\frac{ev_d}{2\cos\theta_W} & \frac{ev_u}{2\cos\theta_W} \\ 0 & M_2 & \frac{ev_d}{2\sin\theta_W} & -\frac{ev_u}{2\sin\theta_W} \\ -\frac{ev_d}{2\cos\theta_W} & \frac{ev_d}{2\sin\theta_W} & 0 & -\mu \\ \frac{ev_u}{2\cos\theta_W} & -\frac{ev_u}{2\sin\theta_W} & -\mu & 0 \end{pmatrix}, \quad (2.11)$$

with M_1 being the bino mass and θ_W being the weak mixing angle, it is diagonalized by $N\mathcal{M}_{\chi^0}N^T = \mathcal{M}_{\chi^0}^{\text{diag}}$.

3 $b \rightarrow s\ell^+\ell^-$ process in RPV-MSSMIS

When research the $b \rightarrow s\ell^+\ell^-$ process in RPV-MSSMIS, we refer to the assumption made in recent works within the RPV-MSSM model [29–33], that $\lambda'_{ij1} = \lambda'_{ij2} = 0$. Thus the tree-level $b \rightarrow s\ell^+\ell^-$ transition exchanging the \tilde{u}_L to generate the operator $(\bar{s}\gamma_\mu P_R b)(\bar{\ell}\gamma^\mu P_L \ell)$ which is undesirable to explain $b \rightarrow s\ell^+\ell^-$ anomalies, can be screened. We scrutinize all the one-loop Feynman diagrams in RPV-MSSMIS. For the box diagrams, there are eleven chargino box diagrams including nine λ' diagrams (figure 1a) and two non- λ' diagrams (figure 1b), fourteen W or charged Higgs (W/H^\pm) box diagrams including ten λ' ones (figure 1c) and four non- λ' ones (figure 1d), and three $4\lambda'$ box diagrams (figure 1e&f). The concrete contributions of these box diagrams are listed below, with the Passarino–Veltman functions D_2 and D_0 defined in Ref. [33].

The contributions of chargino box diagrams to $b \rightarrow s\ell^+\ell^-$ process are given by,

$$\begin{aligned} C_{9,\ell}^{\chi^\pm} = -C_{10,\ell}^{\chi^\pm} = & -\frac{\sqrt{2}\pi^2 i}{2G_F\eta_t e^2} \left(g_2^2 K_{i3} K_{i2}^* V_{m1}^* V_{n1} (g_2 V_{m1} \tilde{\mathcal{V}}_{v\ell}^{\mathcal{I}} - V_{m2} Y_{\ell v}^{\mathcal{I}}) \right. \\ & (g_2 V_{n1}^* \tilde{\mathcal{V}}_{v\ell}^{\mathcal{I}} - V_{n2}^* Y_{\ell v}^{\mathcal{I}}) D_2[m_{\tilde{\nu}_v}^{\mathcal{I}}, m_{\chi_m^\pm}, m_{\chi_n^\pm}, m_{\tilde{u}_{Li}}] \\ & + y_{ui}^2 K_{i3}^* K_{i2} V_{m2}^* V_{n2} (g_2 V_{m1} \tilde{\mathcal{V}}_{v\ell}^{\mathcal{I}} - V_{m2} Y_{\ell v}^{\mathcal{I}}) \\ & (g_2 V_{n1}^* \tilde{\mathcal{V}}_{v\ell}^{\mathcal{I}} - V_{n2}^* Y_{\ell v}^{\mathcal{I}}) D_2[m_{\tilde{\nu}_v}^{\mathcal{I}}, m_{\chi_m^\pm}, m_{\chi_n^\pm}, m_{\tilde{u}_{Li}}] \\ & - \lambda_{v3k}^{\mathcal{I}} \lambda_{v'2k}^{\mathcal{I}*} (g_2 V_{m1}^* \tilde{\mathcal{V}}_{v\ell}^{\mathcal{I}} - V_{m2}^* Y_{\ell v}^{\mathcal{I}}) (g_2 V_{m1} \tilde{\mathcal{V}}_{v'\ell}^{\mathcal{I}} - V_{m2} Y_{\ell v'}^{\mathcal{I}}) D_2[m_{\tilde{\nu}_v}^{\mathcal{I}}, m_{\tilde{\nu}_{v'}}^{\mathcal{I}}, m_{\chi_m^\pm}, m_{d_k}] \\ & - \tilde{\lambda}_{\ell ik}' \tilde{\lambda}_{\ell jk}^{\mathcal{I}*} g_2^2 K_{i3} K_{j2}^* |V_{m1}|^2 D_2[m_{\tilde{u}_{Li}}, m_{\tilde{u}_{Lj}}, m_{\chi_m^\pm}, m_{d_k}] \\ & + \tilde{\lambda}_{\ell ik}' \lambda_{v2k}^{\mathcal{I}*} (g_2 K_{i3} V_{m1}^*) (g_2 V_{m1} \tilde{\mathcal{V}}_{v\ell}^{\mathcal{I}} - V_{m2} Y_{\ell v}^{\mathcal{I}}) D_2[m_{\tilde{\nu}_v}^{\mathcal{I}}, m_{\tilde{u}_{Li}}, m_{\chi_m^\pm}, m_{d_k}] \\ & \left. + \tilde{\lambda}_{\ell ik}'^* \lambda_{v3k}^{\mathcal{I}} (g_2 K_{i2}^* V_{m1}) (g_2 V_{m1}^* \tilde{\mathcal{V}}_{v\ell}^{\mathcal{I}} - V_{m2}^* Y_{\ell v}^{\mathcal{I}}) D_2[m_{\tilde{\nu}_v}^{\mathcal{I}}, m_{\tilde{u}_{Li}}, m_{\chi_m^\pm}, m_{d_k}] \right), \quad (3.1) \end{aligned}$$

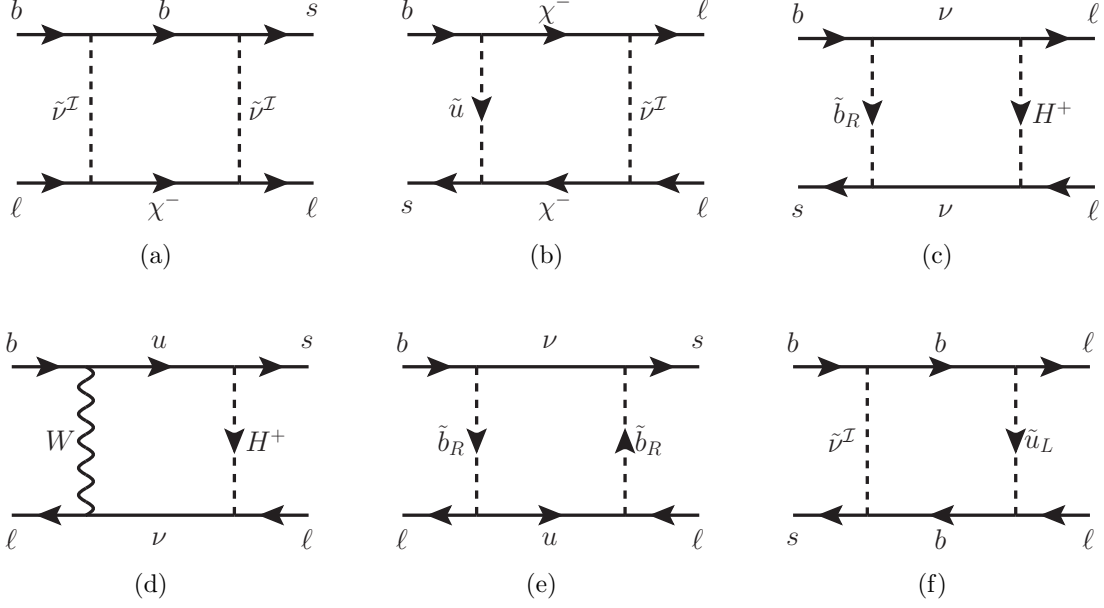


Figure 1: Box diagrams for $b \rightarrow s\ell^+\ell^-$ process in our parameter scheme. Figure (a) and figure (b) show one example of λ' diagrams and non- λ' diagrams of chargino box, respectively. Figure (c) and figure (d) show one example of λ' diagrams and non- λ' diagrams of W/H^\pm box, respectively. Figure (e) and (f) are the three $4\lambda'$ box diagrams with the $\tilde{\nu}^{\mathcal{R}}$ -engaged diagram omitted.

where the Yukawa coupling $y_{u_i} = \sqrt{2}m_{u_i}/v_u$ and $Y_{\ell v}^{\mathcal{I}} = (Y_\nu)_{j\ell} \tilde{\mathcal{Y}}_{v(j+3)}^{\mathcal{I}*}$, and $\ell = 1, 2$ denoting the electron and muon flavour respectively in equations all through this paper.

The contributions of W/H^\pm box diagrams to $b \rightarrow s\ell^+\ell^-$ process are given by,

$$\begin{aligned}
C_{9,\ell}^{W/H^\pm} = -C_{10,\ell}^{W/H^\pm} = & -\frac{\sqrt{2}\pi^2 i}{2G_F\eta_t e^2} \left(y_{u_i}^2 K_{i3} K_{i2}^* Z_{H_{h2}}^2 Z_{H_{h'2}}^2 |Y_{\ell v}^{\mathcal{N}}|^2 D_2[m_{\nu_v}, m_{u_i}, m_{H_h}, m_{H_{h'}}] \right. \\
& - 4g_2^2 m_{u_i} y_{u_i} m_{\nu_v} K_{i3} K_{i2}^* Z_{H_{h2}}^2 \text{Re}(\mathcal{V}_{v\ell} Y_{\ell v}^{\mathcal{N}*}) D_0[m_{\nu_v}, m_{u_i}, m_W, m_{H_h}] \\
& + 5g_2^4 K_{i3} K_{i2}^* |\mathcal{V}_{v\ell}|^2 D_2[m_{\nu_v}, m_{u_i}, m_W, m_W] \\
& + Z_{H_{h2}}^2 Y_{\ell v}^{\mathcal{N}*} Y_{\ell v'}^{\mathcal{N}} \lambda_{v'3k}' \lambda_{v'2k}^{\mathcal{N}*} D_2[m_{\nu_v}, m_{\nu_{v'}}, m_{H_h}, m_{\tilde{d}_{Rk}}] \\
& - 2g_2^2 m_{\nu_v} m_{\nu_{v'}} \mathcal{V}_{v\ell}^* \mathcal{V}_{v'\ell} \lambda_{v'3k}' \lambda_{v'2k}^{\mathcal{N}*} D_0[m_{\nu_v}, m_{\nu_{v'}}, m_W, m_{\tilde{d}_{Rk}}] \\
& + 2m_{\nu_v} m_{\nu_{v'}} Z_{H_{h2}}^2 Y_{\ell v}^{\mathcal{N}} Y_{\ell v'}^{\mathcal{N}*} \lambda_{v'3k}' \lambda_{v'2k}^{\mathcal{N}*} D_0[m_{\nu_v}, m_{\nu_{v'}}, m_{H_h}, m_{\tilde{d}_{Rk}}] \\
& + 2m_{u_i} m_{u_j} y_{u_i} y_{u_j} K_{i3} K_{j2}^* Z_{H_{h2}}^2 \tilde{\lambda}_{\ell ik}' \tilde{\lambda}_{\ell jk}^{\mathcal{I}*} D_0[m_{u_i}, m_{u_j}, m_{H_h}, m_{\tilde{d}_{Rk}}] \\
& - g_2^2 \mathcal{V}_{v\ell} \mathcal{V}_{v'\ell}^* \lambda_{v'3k}' \lambda_{v'2k}^{\mathcal{N}*} D_2[m_{\nu_v}, m_{\nu_{v'}}, m_W, m_{\tilde{d}_{Rk}}] \\
& - g_2^2 K_{i3} K_{j2}^* \tilde{\lambda}_{\ell ik}' \tilde{\lambda}_{\ell jk}^{\mathcal{I}*} D_2[m_{u_i}, m_{u_j}, m_W, m_{\tilde{d}_{Rk}}] \\
& - 2m_{u_i} y_{u_i} m_{\nu_v} K_{i3} Z_{H_{h2}}^2 Y_{\ell v}^{\mathcal{N}*} \tilde{\lambda}_{\ell ik}' \lambda_{v'2k}^{\mathcal{N}*} D_0[m_{u_i}, m_{\nu_v}, m_{H_h}, m_{\tilde{d}_{Rk}}] \\
& \left. - 2m_{u_i} y_{u_i} m_{\nu_v} K_{i2}^* Z_{H_{h2}}^2 Y_{\ell v}^{\mathcal{N}} \tilde{\lambda}_{\ell ik}^{\mathcal{I}*} \lambda_{v'3k}' D_0[m_{u_i}, m_{\nu_v}, m_{H_h}, m_{\tilde{d}_{Rk}}] \right)
\end{aligned}$$

$$\begin{aligned}
& + g_2^2 K_{i2}^* \mathcal{V}_{v\ell} \tilde{\lambda}_{\ell ik}'^* \lambda_{v3k}'^{\mathcal{N}} D_2[m_{u_i}, m_{\nu_v}, m_W, m_{\tilde{d}_{Rk}}] \\
& + g_2^2 K_{i3} \mathcal{V}_{v\ell}^* \tilde{\lambda}_{\ell ik}' \lambda_{v2k}'^{\mathcal{N}*} D_2[m_{u_i}, m_{\nu_v}, m_W, m_{\tilde{d}_{Rk}}] \Big), \tag{3.2}
\end{aligned}$$

where the mixing matrix elements $Z_{H12} = -\sin \beta$, $Z_{H22} = -\cos \beta$ with Goldstone mass $m_{H_1} = m_W$ and changed Higgs mass $m_{H_2} = m_{H^\pm}$ and $Y_{\ell v}^{\mathcal{N}} = (Y_\nu)_{j\ell} \mathcal{V}_{v(j+3)}^*$.

The contributions of $4\lambda'$ box diagrams to $b \rightarrow s\ell^+\ell^-$ process are given by,

$$\begin{aligned}
C_{9,\ell}^{4\lambda'} = -C_{10,\ell}^{4\lambda'} = & -\frac{\sqrt{2}\pi^2 i}{2G_F \eta_t e^2} \left(\tilde{\lambda}_{\ell ik}' \tilde{\lambda}_{\ell ik}'^* \lambda_{v3k}'^{\mathcal{N}} \lambda_{v2k}'^{\mathcal{N}*} D_2[m_{\nu_v}, m_{u_i}, m_{\tilde{d}_{Rk}}, m_{\tilde{d}_{Rk}}] \right. \\
& \left. + \tilde{\lambda}_{\ell ik}' \tilde{\lambda}_{\ell ik}'^* \lambda_{v3k}^{\mathcal{I}} \lambda_{v2k}^{\mathcal{I}*} D_2[m_{\tilde{\nu}_v}, m_{\tilde{u}_{Li}}, m_{d_k}, m_{d_k}] \right). \tag{3.3}
\end{aligned}$$

In the following we make the assumption that the mass of RH sbottom, $m_{\tilde{b}_R}$ is sufficiently heavy to focus on the contributions of sneutrinos as the bridge between the trilinear RPV term and the inverse seesaw mechanism, so contributions of sbottoms without sneutrinos are negligible and can be removed. Besides, we also set the masses of LH su-quarks, $m_{\tilde{u}_L}$ adequate heavy³. Because the LFU violating contributions mainly from $\mu^+\mu^-$ channel in box diagrams are expected to explain $b \rightarrow s\ell^+\ell^-$ anomalies in both scenario A and scenario B, we will set that $\mathcal{M}_{\tilde{\nu}^{\mathcal{I}(\mathcal{R})}}^2$ has no flavour mixing and the electron-flavour elements with LH and RH chiralities are both sufficiently heavy. This structure can be achieved by setting all the blocks in mass matrix square diagonal as well as heavy $m_{\tilde{L}_1}^2$ and $m_{\tilde{R}_1}^2$ in Eq. (2.7). Also λ'_{1jk} is set to be zero for simplicity principle. Then nearly all box contributions to $b \rightarrow se^+e^-$ transition and some box contributions to $b \rightarrow s\mu^+\mu^-$ transition can be eliminated and afterwards we show which contributions are remained valid.

Firstly among these remained chargino box diagrams, the non- λ' one with RH sneutrinos previously discussed in Ref. [35] is recalculated by us. We find the Wilson coefficient C_9^{NP} from this diagram equals to $-C_{10}^{\text{NP}}$, different from the $C_9^{\text{NP}} = C_{10}^{\text{NP}}$ of their condition in Ref. [35]. The related C_9^{NP} , namely as $C_V^{\chi^\pm(1)}$ in this paper, is given by

$$\begin{aligned}
C_V^{\chi^\pm(1)} = & -\frac{\sqrt{2}\pi^2 i}{2G_F \eta_t e^2} g_{u_i}^2 K_{i3}^* K_{i2} V_{m2}^* V_{n2} (g_2 V_{m1} \tilde{\mathcal{V}}_{v2}^{\mathcal{I}} - V_{m2} Y_{2v}^{\mathcal{I}}) \\
& (g_2 V_{n1}^* \tilde{\mathcal{V}}_{v2}^{\mathcal{I}} - V_{n2}^* Y_{2v}^{\mathcal{I}}) D_2[m_{\tilde{\nu}_v}^{\mathcal{I}}, m_{\chi_m^\pm}, m_{\chi_n^\pm}, m_{\tilde{u}_{Ri}}]. \tag{3.4}
\end{aligned}$$

We can see that this formula is from the second term of Eq (3.1).

³In this work, $m_{\tilde{b}_R}$ and $m_{\tilde{u}_L}$ are set as around 10 TeV.

Then we show the λ' within chargino box diagram containing the RPV interactions between singlet sneutrinos with quarks. The contribution is given by,

$$C_V^{\chi^\pm(2)} = \frac{\sqrt{2}\pi^2 i}{2G_F \eta_t e^2} \lambda_{v3k}^{\mathcal{I}} \lambda_{v'2k}^{\mathcal{I}*} (g_2 V_{m1}^* \tilde{\mathcal{V}}_{v2}^{\mathcal{I}} - V_{m2}^* Y_{2v}^{\mathcal{I}}) \\ (g_2 V_{m1} \tilde{\mathcal{V}}_{v'2}^{\mathcal{I}} - V_{m2} Y_{2v'}^{\mathcal{I}}) D_2[m_{\tilde{\nu}_v}^{\mathcal{I}}, m_{\tilde{\nu}_{v'}}^{\mathcal{I}}, m_{\chi_m^\pm}, m_{d_k}], \quad (3.5)$$

which is from the third term of Eq (3.1).

The remained W/H^\pm box contributions in Eq. (3.2) are,

$$C_{9,\ell}^{W/H^\pm(1)} = -C_{10,\ell}^{W/H^\pm(1)} = -\frac{\sqrt{2}\pi^2 i}{2G_F \eta_t e^2} \left(y_{u_i}^2 K_{i3} K_{i2}^* Z_{H_{h2}}^2 Z_{H_{h'2}}^2 |Y_{\ell v}^{\mathcal{N}}|^2 D_2[m_{\nu_v}, m_{u_i}, m_{H_h}, m_{H_{h'}}] \right. \\ \left. - 4g_2^2 m_{u_i} y_{u_i} m_{\nu_v} K_{i3} K_{i2}^* Z_{H_{h2}}^2 \text{Re}(\mathcal{V}_{v\ell} Y_{\ell v}^{\mathcal{N}*}) D_0[m_{\nu_v}, m_{u_i}, m_W, m_{H_h}] \right. \\ \left. + 5g_2^4 K_{i3} K_{i2}^* |\mathcal{V}_{v\ell}|^2 D_2[m_{\nu_v}, m_{u_i}, m_W, m_W] \right), \quad (3.6)$$

which is from the first three terms of Eq. (3.2). It is obvious that these contributions include SM effects, which cannot be separated naively from NP effects because of the generation and chiral mixing of massive neutrinos. In addition, these contributions still contain both the $\mu^+ \mu^-$ channel sector and $e^+ e^-$ channel sector. In the following numerical analyses of section 5, we will further investigate it in detail.

Next we show the valid penguin contributions. Firstly, the Wilson coefficients of Z -boson penguin diagrams are found negligible. While the contributions of photon penguin diagrams are expected non-ignorable which are shown in figure 2, where the λ' diagrams (figure 2a) give

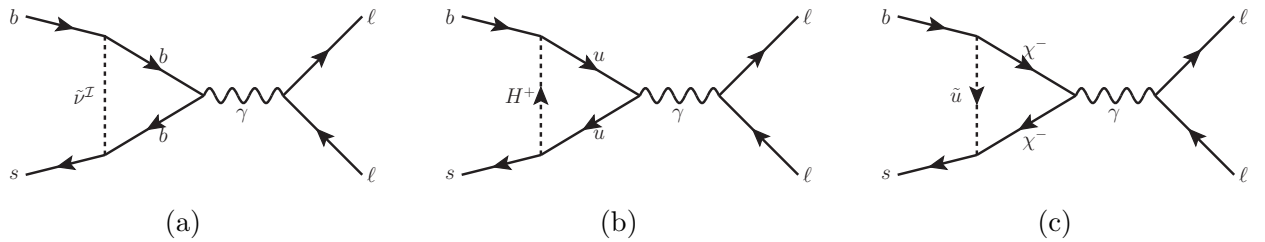


Figure 2: Photon penguin diagrams for $b \rightarrow s \ell^+ \ell^-$ process in our parameter scheme. Figure (a) shows one example of the λ' diagrams. Figure (b) and figure (c) show one example of the non- λ' diagrams with W/H^\pm and charginos engaged respectively.

$$C_U^{\gamma(1)} = -\frac{\sqrt{2}\lambda_{v33}^{\mathcal{I}} \lambda_{v23}^{\mathcal{I}*}}{36G_F \eta_t m_{\tilde{\nu}_v}^2} \left(\frac{4}{3} + \log \frac{m_b^2}{m_{\tilde{\nu}_v}^2} \right), \quad (3.7)$$

while the remained non- λ' contributions (figure 2b&c) named as $C_U^{\gamma(2)}$ are also calculated by us for completeness.

4 The $(g - 2)_\ell$ and other constraints

After the NP effects on $b \rightarrow s\ell^+\ell^-$ process introduced, we discuss the NP effects on $(g - 2)_\ell$ and other related processes.

4.1 The muon (electron) anomalous magnetic moment

The amplitude of the $\ell \rightarrow \ell\gamma$ ($\ell = e, \mu$) transition is given by,

$$i\mathcal{M} = ie\bar{\ell} \left(\gamma^\eta + a_\ell \frac{i\sigma^{\eta\beta} q_\beta}{2m_\ell} \right) \ell A_\eta, \quad (4.1)$$

in the limit of photon moment q tending to zero. The second term in the bracket gives the loop corrections and a_ℓ is called the anomalous magnetic moment for the related lepton.

The one-loop chargino and neutralino contributions in RPV-MSSMIS to a_ℓ are given here, with referring to Ref. [82, 94, 120],

$$\begin{aligned} \delta a_\ell^{\chi^\pm} &= \frac{m_\ell}{16\pi^2} \left[\frac{m_\ell}{6m_{\tilde{\nu}_v}^2} (|c_{mv}^{\ell L}|^2 + |c_{mv}^{\ell R}|^2) F_1^C(m_{\chi_m^\pm}^2/m_{\tilde{\nu}_v}^2) + \frac{m_{\chi_m^\pm}}{m_{\tilde{\nu}_v}^2} \text{Re}[c_{mv}^{\ell L} c_{mv}^{\ell R}] F_2^C(m_{\chi_m^\pm}^2/m_{\tilde{\nu}_v}^2) \right], \\ \delta a_\ell^{\chi^0} &= \frac{m_\ell}{16\pi^2} \left[-\frac{m_\ell}{6m_{\tilde{l}_i}^2} (|n_{ni}^{\ell L}|^2 + |n_{ni}^{\ell R}|^2) F_1^N(m_{\chi_n^0}^2/m_{\tilde{l}_i}^2) + \frac{m_{\chi_n^0}}{m_{\tilde{l}_i}^2} \text{Re}[n_{ni}^{\ell L} n_{ni}^{\ell R}] F_2^N(m_{\chi_n^0}^2/m_{\tilde{l}_i}^2) \right], \end{aligned} \quad (4.2)$$

where,

$$\begin{aligned} c_{mv}^{\ell R} &= y_\ell U_{m2} \tilde{\mathcal{V}}_{v\ell}^{\mathcal{I}}, \quad c_{mv}^{\ell L} = -g_2 V_{m1} \tilde{\mathcal{V}}_{v\ell}^{\mathcal{I}} + V_{m2} Y_{\ell v}^{\mathcal{I}}; \\ n_{ni}^{\ell R} &= \sqrt{2} g_1 N_{n1} \delta_{i(\ell+3)} + y_\ell N_{n3} \delta_{i\ell}, \quad n_{ni}^{\ell L} = \frac{1}{\sqrt{2}} (g_2 N_{n2} + g_1 N_{n1}) \delta_{i\ell} - y_\ell N_{n3} \delta_{i(\ell+3)}, \end{aligned} \quad (4.3)$$

and the factors,

$$\begin{aligned} F_1^C(x) &= \frac{1}{(1-x)^4} (2 + 3x - 6x^2 + x^3 + 6x \log x), \\ F_2^C(x) &= -\frac{1}{(1-x)^3} (3 - 4x + x^2 + 2 \log x), \\ F_1^N(x) &= \frac{1}{(1-x)^4} (1 - 6x + 3x^2 + 2x^3 - 6x^2 \log x), \end{aligned}$$

$$F_2^N(x) = \frac{1}{(1-x)^3} (1 - x^2 + 2x \log x). \quad (4.4)$$

The flavour mixing of RH sleptons is not considered here, neither is the flavour mixing of LH sleptons when LH sneutrinos set diagonal. The contributions from λ' diagrams can be vanished for the heavy \tilde{b}_R and \tilde{u}_L , so they are not shown in Eq. (4.3). Thus the remained NP contributions are just from the inverse seesaw sector. The difference from MSSM is the form factor $c_{mv}^{\ell L}$ in Eq. (4.3), where the extra $V_{m2} Y_{\ell v}^{\mathcal{I}}$ term can give a large enhancement to a_ℓ . Because of the measured Δa_e having different features compared with Δa_μ , we consider the scheme of $|\delta a_\mu^{\chi^\pm}| \gg |\delta a_e^{\chi^\pm}| \approx 0$ and $|\delta a_e^{\chi^0}| \gg |\delta a_\mu^{\chi^0}| \approx 0$ [88], thus, the muon generation of RH sleptons is set sufficient heavy as well as heavy \tilde{L}'_1 which is already assumed in section 3.

4.2 The related constraints

On account of the assumption of heavy \tilde{b}_R , the neutral current processes $B \rightarrow K^{(*)} \nu \bar{\nu}$, $B \rightarrow \pi \nu \bar{\nu}$, $K \rightarrow \pi \nu \bar{\nu}$, $D^0 \rightarrow \mu^+ \mu^-$ and $\tau \rightarrow \mu \rho^0$ as well as the charged current processes $B \rightarrow \tau \nu$, $D_s \rightarrow \tau \nu$ and $\tau \rightarrow K \nu$, which are all the transitions exchanging \tilde{b}_R at tree level, will give no effective constraints.

At one-loop level, the photon penguin diagrams in figure 2 also contribute to the electromagnetic dipole operator $\mathcal{O}_7^{(\prime)} = \frac{m_b}{e} (\bar{s} \sigma^{\mu\nu} P_{R(L)} b) F_{\mu\nu}$ constrained by the $B \rightarrow X_s \gamma$ decay. Large $\tan \beta$ is benefit for suppressing the non- λ' contributions in this work to $B \rightarrow X_s \gamma$ decay [36]. When $\tan \beta$ is large, the Wilson coefficient C_7 is mainly given by $C_7^{\text{NP}} = \sqrt{2} \lambda_{v33}^{\mathcal{I}} \lambda_{v23}^{\mathcal{I}*} / (144 G_F \eta_t m_{\tilde{\nu}_v^{\mathcal{I}}}^2)$ and $C_7'^{\text{NP}}$ is negligible. Compared with $C_U^{\gamma(1)}$ in Eq. (3.7), C_7^{NP} contains the common part $\lambda_{v33}^{\mathcal{I}} \lambda_{v23}^{\mathcal{I}*} / m_{\tilde{\nu}_v^{\mathcal{I}}}^2$ while no logarithmic term. The recent measurements of branching ratio $\mathcal{B}(B \rightarrow X_s \gamma)_{\text{exp}} \times 10^4 = 3.43 \pm 0.21 \pm 0.07$ [50], consist with the SM prediction $\mathcal{B}(B \rightarrow X_s \gamma)_{\text{SM}} \times 10^4 = 3.36 \pm 0.23$ [121], induce the bound [34] to

$$\left| \frac{\lambda_{v33}^{\mathcal{I}} \lambda_{v23}^{\mathcal{I}*}}{(m_{\tilde{\nu}_v^{\mathcal{I}}} / 1 \text{TeV})^2} \right| \lesssim 1.25, \quad (4.5)$$

and ones can see that the constraints will be weak when there is the cancellation within the left absolute value sign of Eq. (4.5).

Another process we should consider is $B_s - \bar{B}_s$ mixing, mastered by the Lagrangian,

$$\mathcal{L} = (C_{B_s}^{\text{SM}} + C_{B_s}^{\text{NP}}) (\bar{s} \gamma_\mu P_L b) (\bar{s} \gamma^\mu P_L b) + \text{h.c.}, \quad (4.6)$$

where the NP contribution is given by

$$C_{B_s}^{\text{NP}} = -\frac{i}{8} \left(\lambda'_{v33} \lambda'_{v23} \lambda'_{v'33} \lambda'_{v'23} D_2[m_{\tilde{\nu}_v^{\mathcal{I}}}, m_{\tilde{\nu}_{v'}^{\mathcal{I}}}, m_b, m_b] \right. \\ \left. + y_{u_i}^2 y_{u_j}^2 (K_{i3}^* K_{i2}) (K_{j3}^* K_{j2}) |V_{m2} V_{n2}|^2 D_2[m_{\chi_m^\pm}, m_{\chi_n^\pm}, m_{\tilde{u}_{Ri}}, m_{\tilde{u}_{Rj}}] \right), \quad (4.7)$$

including the λ' diagram with double sneutrinos and the non- λ' diagram with double RH su-quarks, and the SM contribution $C_{B_s}^{\text{SM}} = -\frac{1}{4\pi^2} G_F^2 m_W^2 \eta_t^2 S(x_t)$ with the function $S(x_t) = \frac{x_t(4-11x_t+x_t^2)}{4(x_t-1)^2} + \frac{3x_t^3 \log(x_t)}{2(x_t-1)^3}$. With the measurement of $\Delta M_s^{\text{exp}} = (17.757 \pm 0.021) \text{ ps}^{-1}$ [122]⁴, the recent SM prediction $\Delta M_s^{\text{SM}} = (18.4_{-1.2}^{+0.7}) \text{ ps}^{-1} = (1.04_{-0.07}^{+0.04}) \Delta M_s^{\text{exp}}$ [124] leads to the bound of

$$0.90 < |1 + C_{B_s}^{\text{NP}}/C_{B_s}^{\text{SM}}| < 1.11, \quad (4.8)$$

at 2σ level.

Then we discuss the lepton flavour violating decays including $l \rightarrow \ell \gamma$, $l \rightarrow \ell \ell \ell$ and $\tau \rightarrow \ell' \ell \ell$, where $l = \tau, \mu$ and $\ell^{(\prime)} = \mu, e$ and $l \neq \ell$. Firstly, the λ' diagrams are only contained in these processes $\tau \rightarrow \mu \gamma$ and $\tau \rightarrow \mu \mu \mu$ given λ'_{1jk} is set to be zero. The related contributions can be eliminated when \tilde{b}_R is sufficient heavy [33]. As to the non- λ' diagrams, the neutralino-slepton diagrams all contain the flavour mixing of sleptons and the chargino-sneutrino diagrams all contain the flavour mixing of sneutrinos (see Ref. [125] for concrete formulas). So the effects of the two kinds of diagrams are vanished when there are no flavour mixing in the mass matrices of sleptons and sneutrinos. For contributions of W/H^\pm -neutrino diagrams, they are all connected to three terms which are $\mathcal{V}_{(\alpha+3)v}^{T*} \mathcal{V}_{(\beta+3)v}^T$, $\mathcal{V}_{(\alpha+3)v}^{T*} \mathcal{V}_{\beta v}^T$ and $\mathcal{V}_{\alpha v}^{T*} \mathcal{V}_{\beta v}^T$ with their conjugate terms omitted, where $\alpha, \beta = e, \mu, \tau$ and $\alpha \neq \beta$ [125]. In the next section, we will show all these terms make no effects under the particular structure of neutrino mass matrix. The same analyses can also be applied to the non- λ' diagrams in $B_s^0 \rightarrow \tau^\pm \mu^\mp$ and $B^+ \rightarrow K^+ \tau^\pm \mu^\mp$. For the λ' diagrams, we refer to the detailed discussions in Ref. [32], in which they found no obvious constraints.

⁴The newly updated experimental result of ΔM_s by LHCb has been reported [123]. The combined result with previous LHCb measurements gives $\Delta M_s^{\text{LHCb}} = (17.7656 \pm 0.0057) \text{ ps}^{-1}$ with the improved precision. Using this new combined result will not change the Eq. (4.8).

5 Numerical analyses

In this section, we investigate $b \rightarrow s\ell^+\ell^-$ anomalies numerically as well as the a_μ anomaly and the related constraints introduced in section 4.

We adopt the diagonal Yukawa $Y_\nu = \text{diag}(0.7, 0.8, 0.5)$ [47] and the diagonal M_R with the element value of 1 TeV, then μ_S can be expressed by m_D , M_R , U^{PMNS} and the light neutrino masses $m_\nu^{\text{diag}} \approx \text{diag}(0, \sqrt{\Delta m_{21}^2}, \sqrt{\Delta m_{31}^2 + \Delta m_{21}^2})$ with the normal mass ordering [126] using Eq. (2.5). The CP violation is not considered in U^{PMNS} so $\delta_{\text{CP}} = \pi$ which is accord with the normal mass ordering [44]. The exact physics masses of light neutrinos are gotten as $\text{diag}(0, 0.008, 0.05)$ eV from the data in Ref. [44], with heavy neutrino physics masses with the value of around 1 TeV. The approximate numerical form of the mixing matrix \mathcal{V}^T is given,

$$\mathcal{V}^T \approx \begin{pmatrix} 0.841 & 0.507 & -0.147 & -0.084i & 0 & 0 & 0.084 & 0 & 0 \\ -0.230 & 0.599 & 0.755 & 0 & 0.096i & 0 & 0 & 0.096 & 0 \\ 0.477 & -0.609 & 0.629 & 0 & 0 & 0.060i & 0 & 0 & -0.060 \\ 0 & 0 & 0 & 0.707i & 0 & 0 & 0.707 & 0 & 0 \\ 0 & 0 & 0 & 0 & -0.707i & 0 & 0 & 0.707 & 0 \\ 0 & 0 & 0 & 0 & 0 & -0.707i & 0 & 0 & -0.707 \\ -0.101 & -0.061 & 0.018 & -0.702i & 0 & 0 & 0.702 & 0 & 0 \\ 0.032 & -0.082 & -0.104 & 0 & 0.701i & 0 & 0 & 0.701 & 0 \\ -0.041 & 0.052 & -0.054 & 0 & 0 & 0.705i & 0 & 0 & -0.705 \end{pmatrix}. \quad (5.1)$$

Ones can see that the light generation sector $\mathcal{V}_{ij}^{T^{3 \times 3}}$ approximate U_{ij}^{PMNS} , and furthermore there is no flavour mixing when RH sector engaged but chiral mixing exists. With the numerical result of Eq. (5.1), ones can see that $\mathcal{V}_{(\alpha+3)v}^{T*} \mathcal{V}_{(\beta+3)v}^T$ and $\mathcal{V}_{(\alpha+3)v}^{T*} \mathcal{V}_{\beta v}^T$ in the contributions of W/H^\pm -neutrino diagrams to the lepton flavour violating decays within section 4.2 are eliminated. $\mathcal{V}_{\alpha v}^{T*} \mathcal{V}_{\beta v}^T$ can be decomposed into the following two parts, $\sum_{v_h=4}^9 \mathcal{V}_{\alpha v_h}^{T*} \mathcal{V}_{\beta v_h}^T$ and $\sum_{i=1}^3 \mathcal{V}_{\alpha i}^{T*} \mathcal{V}_{\beta i}^T = -\sum_{v_h=4}^9 \mathcal{V}_{\alpha v_h}^{T*} \mathcal{V}_{\beta v_h}^T$ related to the nearly degenerate heavy neutrinos and light neutrinos respectively [119]. It can be found that $\mathcal{V}_{\alpha v}^{T*} \mathcal{V}_{\beta v}^T$ make no effects. Then we discuss the feature of $C_{9(10),\ell}^{W/H^\pm(1)}$ in Eq. (3.6) in the following.

The three terms of Eq. (3.6) contain $|\mathcal{V}_{(\ell+3)v}^T|^2$, $\text{Re}(\mathcal{V}_{\ell v}^T \mathcal{V}_{(\ell+3)v}^T)$ and $|\mathcal{V}_{\ell v}^T|^2$ respectively. For h or/and $h' = 2$ firstly, this part of Eq. (3.6) includes the contribution of charged Higgs and it can

be ignored when $\tan \beta$ is large. We set $\tan \beta = 6.12$ as Ref. [47]. Then for $h = h' = 1$, this part of Eq. (3.6) is the contribution of seesaw-extended SM. $|\mathcal{V}_{\ell v}^T|^2$ in the third term is dominated by $|U_{\ell i}^{\text{PMNS}}|^2$ and so this term is nearly equal to the contribution of the original SM without being extended. Because $\text{Re}(\mathcal{V}_{\ell v}^T \mathcal{V}_{(\ell+3)v}^T)$ is negligible compared with $|\mathcal{V}_{(\ell+3)v}^T|^2$, we focus on the first term in Eq. (3.6) and the second term can be omitted safely. According to the discussion above, the pure NP contribution $\Delta C_{9(10),\ell}^{W/H^\pm}$ from Eq. (3.6) is given by

$$\Delta C_{9,\ell}^{W/H^\pm} = -\frac{\sqrt{2}\pi^2 i}{2G_F \eta_t e^2} y_{u_i}^2 K_{i3} K_{i2}^* \sin^4 \beta |Y_{\nu \ell} \mathcal{V}_{v(\ell+3)}|^2 D_2[m_{\nu_v}, m_{u_i}, m_W, m_W]. \quad (5.2)$$

Similar to the heavy sector of \mathcal{V}^T , the sneutrino mixing matrices $\tilde{\mathcal{V}}^{\mathcal{I}(\mathcal{R})}$ should only have chiral mixing without flavour mixing because of the discussions in section 4. We set the blocks $m_{\tilde{L}'}, m_{\tilde{R}}^2, B_{M_R}$ and A_ν in Eq. (2.7) all diagonal furthermore. Especially, we set $m_{\tilde{L}'_1} = 5$ TeV equalling to $m_{\tilde{\mu}_R}$ and $m_{\tilde{R}} = \text{diag}(5, 0, 0)$ TeV for the discussion in section 3 and section 4.1 as well as $B_{M_R} = 0.5 M_R^T M_R$ for the proper chiral mixing scale of sneutrinos. Besides, the assignment is done that $M_2 = 250$ GeV and $\mu = 300$ GeV, as well as $m_{\tilde{u}_{Ri}} = 1500$ GeV [127, 128]. With related parameter values given, We find the contribution $\Delta C_{9,\ell}^{W/H^\pm} = -\Delta C_{10,\ell}^{W/H^\pm}$ in Eq. (5.2) are at negative 10^{-2} scale for both $\mu^+ \mu^-$ and $e^+ e^-$ channel. This small LFU effect cannot be included in both C_V and C_U within Eq. (1.3) and is omitted for the approximation. Also we get $C_U^{\gamma(2)}$ around positive 0.01. Then we can make a summary that the LFU violating coefficient $C_V = C_V^{\chi^\pm(1)} + C_V^{\chi^\pm(2)}$ and the LFU coefficient $C_U = C_U^{\gamma(1)} + C_U^{\gamma(2)}$. We find that the factor $c_{mv}^{\mu L} = -g_2 V_{m1}^* \tilde{\mathcal{V}}_{v2}^{\mathcal{I}} + V_{m2}^* Y_{2v}^{\mathcal{I}}$ in Eq. (4.3) is also within $C_V^{\chi^\pm(1)}$ and $C_V^{\chi^\pm(2)}$. Its contributions get the rough numerical estimation,

$$\sum_{m=1}^2 -g_2 V_{m1}^* \tilde{\mathcal{V}}_{v2}^{\mathcal{I}} + V_{m2}^* Y_{2v}^{\mathcal{I}} \approx 0.24 \tilde{\mathcal{V}}_{v2}^{\mathcal{I}} + 1.09 \tilde{\mathcal{V}}_{v5}^{\mathcal{I}}, \quad (5.3)$$

when chargino masses are nearly degenerate. So the large chiral mixing of sneutrinos will make the enhancement to both C_V and a_μ^{NP} simultaneously.

With various model parameters fixed, the main unfixed parameters are $m_{\tilde{L}'_2}, \lambda'_{223}, \lambda'_{233}, \lambda'_{323}$ and λ'_{333} , then we will search the common area of these variables for explaining $b \rightarrow s \ell^+ \ell^-$ anomalies considering the constraints shown in section 4.2, in two fit scenarios mentioned in section 1.

Scenario A is considered firstly thus C_U should be 0 as the definition. We set $A_\nu = 0$ and

$m_{\tilde{L}'_2} = m_{\tilde{L}'_3} + 50$ GeV, benefit for fulfilling the constraint of $B_s - \bar{B}_s$ mixing. To make C_U cancel, $\lambda'_{323}\lambda'_{333}$ is figured out as the expression of $\lambda'_{223}\lambda'_{233}$ and vice versa, then the constraints from $B_s - \bar{B}_s$ mixing and $B \rightarrow X_s\gamma$ will be mainly suppressed. In figure 3, the common areas of $b \rightarrow s\ell^+\ell^-$ explanations under other bounds show a larger value and region of $\lambda'_{223}\lambda'_{233}$ or $-\lambda'_{323}\lambda'_{333}$ for a heavier $m_{\tilde{L}'_2}$. The values of $\lambda'_{323}\lambda'_{333}$ always have the negative sign compared with the positive $\lambda'_{223}\lambda'_{233}$, and their region sizes are nearly the same for the same value of $m_{\tilde{L}'_2}$. As examples, we get the region $0.08 < \lambda'_{223}\lambda'_{233} < 0.1$ for $m_{\tilde{L}'_2} = 250$ GeV and $0.82 < \lambda'_{223}\lambda'_{233} < 1.13$ for $m_{\tilde{L}'_2} = 900$ GeV in 1σ fit.

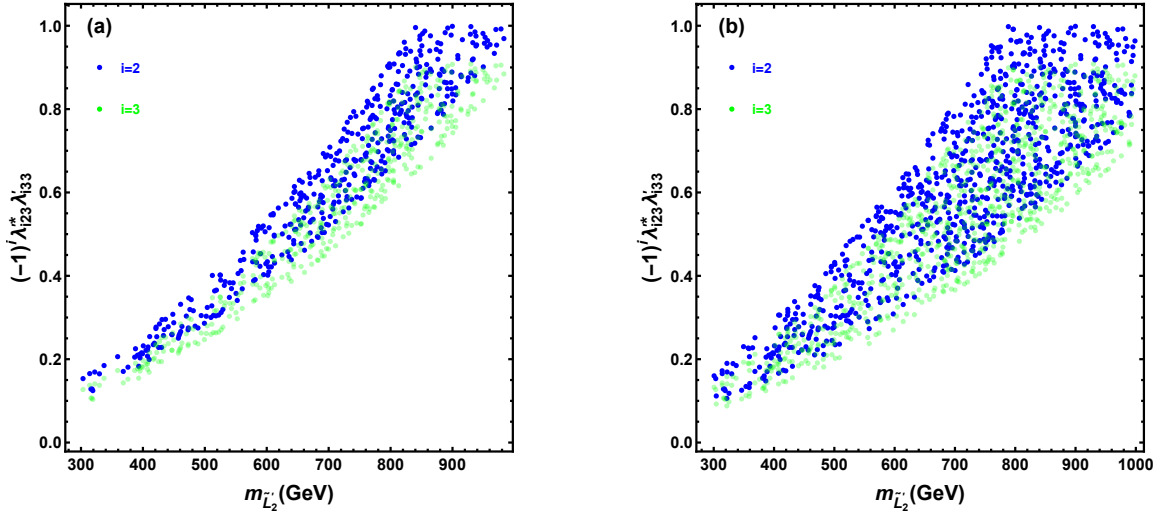


Figure 3: The common scopes of constraints in scenario A. The blue (green) points show $\lambda'_{223}\lambda'_{233}$ ($-\lambda'_{323}\lambda'_{333}$) varies with $m_{\tilde{L}'_2}$ then $\lambda'_{323}\lambda'_{333}$ ($\lambda'_{223}\lambda'_{233}$) is derived. It should be paid attention to that among $\lambda'_{223}\lambda'_{233}$ and $\lambda'_{323}\lambda'_{333}$ there is only one independent variable in this scenario so the blue and green points are relevant practically. The fit level of rare B -meson decays is 1σ in the left panel and 2σ in the right panel.

Then we consider scenario B. We set $A_{\nu\mu} = -1500$ GeV and $m_{\tilde{L}'_2}$ is fixed equalling to $m_{\tilde{L}'_3}$. The common scopes are shown in figure 4 and figure 5. Similar to scenario A, the values of allowed $\lambda'_{323}\lambda'_{333}$ are always negative compared with the positive $\lambda'_{223}\lambda'_{233}$ and the region sizes of their common scopes become larger as $m_{\tilde{L}'_2}$ varying heavier. As shown in figure 4, the $B_s - \bar{B}_s$ mixing constrains mostly while $B \rightarrow X_s\gamma$ decays make no extra bounds. When $m_{\tilde{L}'_2} \lesssim 750$ GeV, the $b \rightarrow s\ell^+\ell^-$ anomalies can be explained at both 1σ and 2σ levels for the B -meson decay fits. When $m_{\tilde{L}'_2}$ reaches around 750 GeV, 1σ explanations will not be viable, however the 2σ ones can be always feasible even when $m_{\tilde{L}'_2}$ at 1 TeV scale. In figure 5(a), we compare the common region sizes for the different fixed $m_{\tilde{L}'_2}$ with each other and find that the deviation between the allowed region size of $\lambda'_{223}\lambda'_{233}$ and $-\lambda'_{323}\lambda'_{333}$ is small, up to around 0.1 scale. Thus

we further fix them equalling to each other and show $\lambda'_{223}\lambda'_{233}$ varying with increasing $m_{\tilde{L}_2}$ in figure 5(b). Compared with the results of scenario A in figure 3, here the 1σ favored fit requires $0.2 \lesssim \lambda'_{223}\lambda'_{233} \lesssim 0.4$ and $m_{\tilde{L}_2} \lesssim 650$ GeV while the region of 2σ fit has a broader size. The common regions in scenario A are both broad for 1 and 2σ fits while it needs some purposeful adjusting of $m_{\tilde{L}_i}$ and λ' parameters while the parameter scheme in scenario B is more natural.

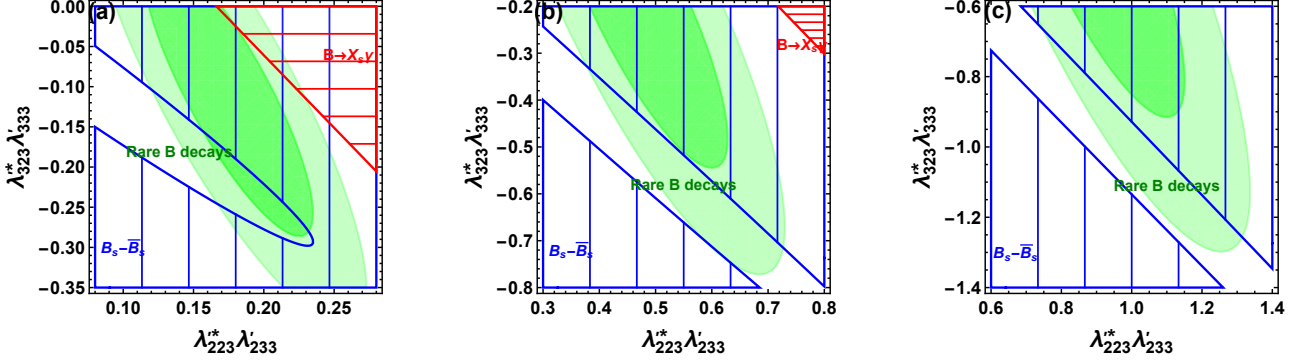


Figure 4: The regions of constraints in scenario B. The green regions are $1(2)\sigma$ favored ones with dark (light) opacity to explain the $b \rightarrow s\ell^+\ell^-$ anomaly. The hatched blue areas are excluded by $B_s - \bar{B}_s$ mixing at 2σ level and the hatched red areas are excluded by $B \rightarrow X_s\gamma$ decays at 2σ level. Besides, $m_{\tilde{L}_3} = m_{\tilde{L}_2}$ are fixed as 500 (left), 750 (middle) and 1000 GeV (right).

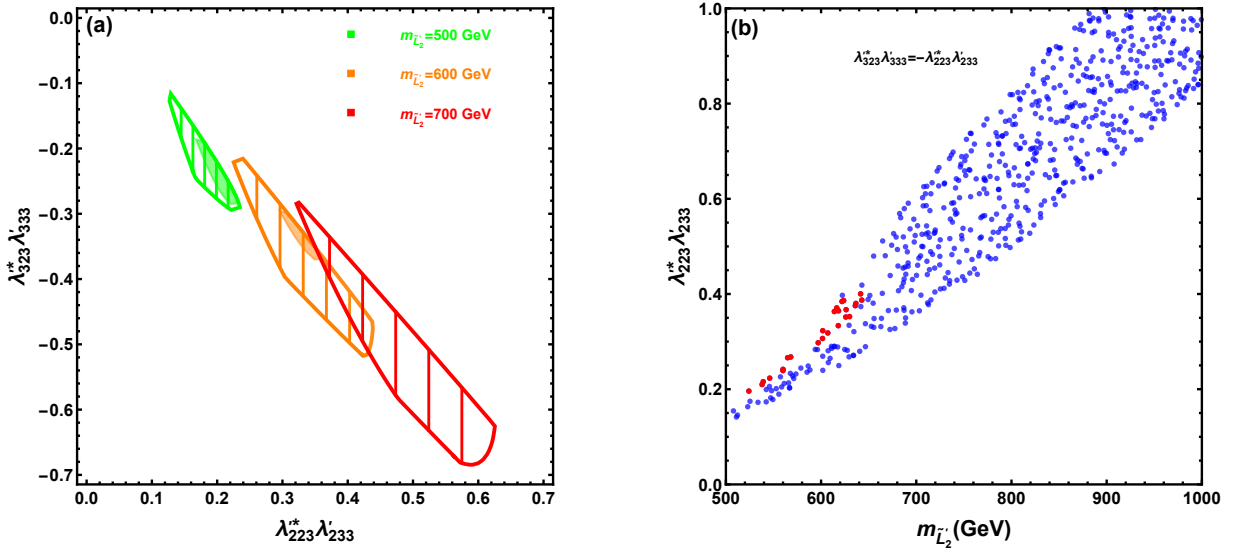


Figure 5: The common scopes of constraints in scenario B. Figure (a): The common scopes are constrained by $b \rightarrow s\ell^+\ell^-$ anomaly fits at 1σ level denoted by painted areas and 2σ level denoted by hatched areas combined with other process constraints at 2σ level for $m_{\tilde{L}_3} = m_{\tilde{L}_2} = 500$ (green), 600 (orange) and 700 GeV (red). Figure (b): The points fulfil $b \rightarrow s\ell^+\ell^-$ anomaly fits with $1(2)\sigma$ favored denoted by red (blue) colour and other process bounds at 2σ level are considered. The assumption is made that $\lambda'_{323}\lambda'_{333} = -\lambda'_{223}\lambda'_{233}$.

Next we will show in both scenario A and B, a_μ^{NP} can make a large positive increasing added to a_μ^{SM} and accommodate the observed 4.2σ deviation, below 2σ level, in figure 6. In scenario A, we get the allowed range $250 \lesssim m_{\tilde{L}'_2} \lesssim 300$ GeV and there is a larger range of $400 \lesssim m_{\tilde{L}'_2} \lesssim 550$ GeV in scenario B. Combining this result with the discussion of $b \rightarrow s\ell^+\ell^-$ anomalies above, we find the $b \rightarrow s\ell^+\ell^-$ and a_μ anomalies can be explained simultaneously in the both of the two scenarios. It should be mentioned that a_e^{NP} can be at negative $\mathcal{O}(10^{-14})$

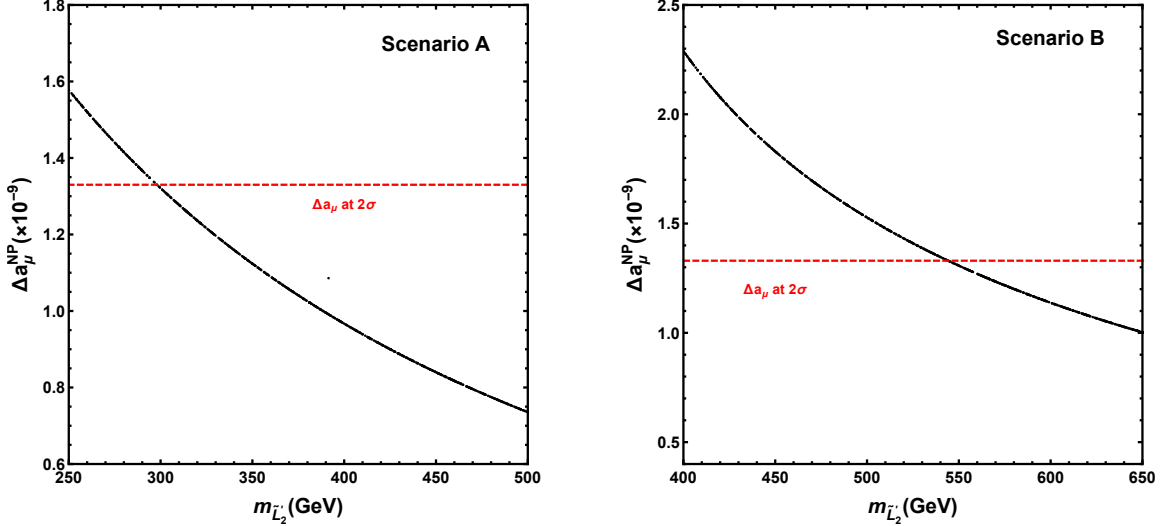


Figure 6: Δa_μ^{NP} varies with $m_{\tilde{L}'_2}$ when $M_1 = M_2 = 250$ GeV in scenario A (left) and scenario B (right).

when M_1 and $m_{\tilde{e}_R}$ are nearly 100 GeV, being not able to reach negative $\mathcal{O}(10^{-13})$ in our parameter spaces.

6 Conclusions

Recent measurements within the transition $b \rightarrow s\ell^+\ell^-$ reveal the deviations from SM predictions. The most motivative R_K anomaly and anomalies from other observables like P'_5 , named $b \rightarrow s\ell^+\ell^-$ anomalies collectively, suggest the new physics of LFU violation may exist. Besides, this NP may also affect the enduring muon anomalous magnetic moment, $(g-2)_\mu$ problem.

In this work, we have studied the chiral mixing effects of sneutrinos in the R -parity violating MSSM with inverse seesaw mechanisms to explore the explanation of $b \rightarrow s\ell^+\ell^-$ anomalies with $(g-2)_\mu$ problem simultaneously. Here all the one-loop contributions to $b \rightarrow s\ell^+\ell^-$ processes are scrutinized under the assumption of $\lambda'_{ij1} = \lambda'_{ij2} = 0$. Among them, the contributions of chiral mixing between LH and singlet (s)neutrinos within superpotential term $\lambda'_{ijk} \hat{L}_i \hat{Q}_j \hat{D}_k$ are

given for the first time to our knowledge. To explain $b \rightarrow s\ell^+\ell^-$ anomalies in this model, two kinds of model-independent global fits are adopted. One is the single-parameter scenario of $C_{9,\mu}^{\text{NP}} = -C_{10,\mu}^{\text{NP}}$ and the other scenario is the double-parameter one that $(\pm)C_V$ contributes to the $C_{9(10),\mu}^{\text{NP}}$ part in $\mu^+\mu^-$ channel and C_U contributes to C_9^{NP} part in both $\mu^+\mu^-$ and e^+e^- channel. Then in the numerical analyses, we find that $b \rightarrow s\ell^+\ell^-$ and $(g-2)_\mu$ anomalies can be explained simultaneously in both scenario A and B. The main constraints among related processes is from $B_s - \bar{B}_s$ mixing covering $B \rightarrow X_s\gamma$ decay and the other tree-level and one-loop processes make no effective bounds.

Acknowledgements

We thank Yi-Lei Tang and Chengfeng Cai for valuable discussions. This work is supported in part by the National Natural Science Foundation of China under Grant No. 11875327, the Fundamental Research Funds for the Central Universities, and the Sun Yat-Sen University Science Foundation.

References

- [1] **LHCb** Collaboration, R. Aaij et al., *Test of lepton universality in beauty-quark decays*, [arXiv:2103.11769](#).
- [2] **LHCb** Collaboration, R. Aaij et al., *Search for lepton-universality violation in $B^+ \rightarrow K^+\ell^+\ell^-$ decays*, *Phys. Rev. Lett.* **122** (2019), no. 19 191801, [[arXiv:1903.09252](#)].
- [3] **LHCb** Collaboration, R. Aaij et al., *Test of lepton universality with $B^0 \rightarrow K^{*0}\ell^+\ell^-$ decays*, *JHEP* **08** (2017) 055, [[arXiv:1705.05802](#)].
- [4] **BELLE** Collaboration, S. Choudhury et al., *Test of lepton flavor universality and search for lepton flavor violation in $B \rightarrow K\ell\ell$ decays*, *JHEP* **03** (2021) 105, [[arXiv:1908.01848](#)].
- [5] **Belle** Collaboration, A. Abdesselam et al., *Test of Lepton-Flavor Universality in $B \rightarrow K^*\ell^+\ell^-$ Decays at Belle*, *Phys. Rev. Lett.* **126** (2021), no. 16 161801, [[arXiv:1904.02440](#)].

- [6] **LHCb** Collaboration, R. Aaij et al., *Measurement of CP-Averaged Observables in the $B^0 \rightarrow K^{*0}\mu^+\mu^-$ Decay*, *Phys. Rev. Lett.* **125** (2020), no. 1 011802, [[arXiv:2003.04831](#)].
- [7] **LHCb** Collaboration, R. Aaij et al., *Angular analysis of the $B^0 \rightarrow K^{*0}\mu^+\mu^-$ decay using 3 fb^{-1} of integrated luminosity*, *JHEP* **02** (2016) 104, [[arXiv:1512.04442](#)].
- [8] **LHCb** Collaboration, R. Aaij et al., *Measurement of Form-Factor-Independent Observables in the Decay $B^0 \rightarrow K^{*0}\mu^+\mu^-$* , *Phys. Rev. Lett.* **111** (2013) 191801, [[arXiv:1308.1707](#)].
- [9] **CMS** Collaboration, V. Khachatryan et al., *Angular analysis of the decay $B^0 \rightarrow K^{*0}\mu^+\mu^-$ from pp collisions at $\sqrt{s} = 8\text{ TeV}$* , *Phys. Lett.* **B753** (2016) 424–448, [[arXiv:1507.08126](#)].
- [10] **ATLAS** Collaboration, M. Aaboud et al., *Angular analysis of $B_d^0 \rightarrow K^{*}\mu^+\mu^-$ decays in pp collisions at $\sqrt{s} = 8\text{ TeV}$ with the ATLAS detector*, *JHEP* **10** (2018) 047, [[arXiv:1805.04000](#)].
- [11] **Belle** Collaboration, S. Wehle et al., *Lepton-Flavor-Dependent Angular Analysis of $B \rightarrow K^{*}\ell^+\ell^-$* , *Phys. Rev. Lett.* **118** (2017), no. 11 111801, [[arXiv:1612.05014](#)].
- [12] **Belle** Collaboration, A. Abdesselam et al., *Angular analysis of $B^0 \rightarrow K^{*}(892)^0\ell^+\ell^-$* , in *Proceedings, LHCSki 2016 - A First Discussion of 13 TeV Results: Obergurgl, Austria, April 10-15, 2016*, 2016. [arXiv:1604.04042](#).
- [13] J. Aebischer, W. Altmannshofer, D. Guadagnoli, M. Reboud, P. Stangl, and D. M. Straub, *B-decay discrepancies after Moriond 2019*, *Eur. Phys. J. C* **80** (2020), no. 3 252, [[arXiv:1903.10434](#)].
- [14] A. K. Alok, A. Dighe, S. Gangal, and D. Kumar, *Continuing search for new physics in $b \rightarrow s\mu\mu$ decays: two operators at a time*, *JHEP* **06** (2019) 089, [[arXiv:1903.09617](#)].
- [15] M. Algueró, B. Capdevila, A. Crivellin, S. Descotes-Genon, P. Masjuan, J. Matias, and J. Virto, *Emerging patterns of New Physics with and without Lepton Flavour Universal contributions*, *Eur. Phys. J.* **C79** (2019), no. 8 714, [[arXiv:1903.09578](#)].

- [16] M. Ciuchini, A. M. Coutinho, M. Fedele, E. Franco, A. Paul, L. Silvestrini, and M. Valli, *New Physics in $b \rightarrow s\ell^+\ell^-$ confronts new data on Lepton Universality*, *Eur. Phys. J. C* **79** (2019), no. 8 719, [[arXiv:1903.09632](#)].
- [17] A. Arbey, T. Hurth, F. Mahmoudi, D. M. Santos, and S. Neshatpour, *Update on the $b \rightarrow s$ anomalies*, *Phys. Rev. D* **100** (2019), no. 1 015045, [[arXiv:1904.08399](#)].
- [18] K. Kowalska, D. Kumar, and E. M. Sessolo, *Implications for new physics in $b \rightarrow s\mu\mu$ transitions after recent measurements by Belle and LHCb*, *Eur. Phys. J. C* **79** (2019), no. 10 840, [[arXiv:1903.10932](#)].
- [19] B. Capdevila, U. Laa, and G. Valencia, *Fitting in or odd one out? Pulls vs residual responses in $b \rightarrow s\ell^+\ell^-$* , [arXiv:1908.03338](#).
- [20] S. Bhattacharya, A. Biswas, S. Nandi, and S. K. Patra, *Exhaustive model selection in $b \rightarrow s\ell\ell$ decays: Pitting cross-validation against the Akaike information criterion*, *Phys. Rev. D* **101** (2020), no. 5 055025, [[arXiv:1908.04835](#)].
- [21] L.-S. Geng, B. Grinstein, S. Jäger, S.-Y. Li, J. Martin Camalich, and R.-X. Shi, *Implications of new evidence for lepton-universality violation in $b \rightarrow s\ell^+\ell^-$ decays*, [arXiv:2103.12738](#).
- [22] W. Altmannshofer and P. Stangl, *New Physics in Rare B Decays after Moriond 2021*, [arXiv:2103.13370](#).
- [23] C. Cornella, D. A. Faroughy, J. Fuentes-Martín, G. Isidori, and M. Neubert, *Reading the footprints of the B-meson flavor anomalies*, [arXiv:2103.16558](#).
- [24] M. Algueró, B. Capdevila, S. Descotes-Genon, J. Matias, and M. Novoa-Brunet, *$b \rightarrow s\ell\ell$ global fits after Moriond 2021 results*, in *55th Rencontres de Moriond on Electroweak Interactions and Unified Theories*, 4, 2021. [arXiv:2104.08921](#).
- [25] T. Hurth, F. Mahmoudi, D. M. Santos, and S. Neshatpour, *More Indications for Lepton Nonuniversality in $b \rightarrow s\ell^+\ell^-$* , [arXiv:2104.10058](#).
- [26] **LHCb** Collaboration, R. Aaij et al., *Angular Analysis of the $B^+ \rightarrow K^{*+}\mu^+\mu^-$ Decay*, *Phys. Rev. Lett.* **126** (2021), no. 16 161802, [[arXiv:2012.13241](#)].

- [27] **CMS** Collaboration, A. M. Sirunyan et al., *Measurement of properties of $B_s^0 \rightarrow \mu^+ \mu^-$ decays and search for $B^0 \rightarrow \mu^+ \mu^-$ with the CMS experiment*, *JHEP* **04** (2020) 188, [[arXiv:1910.12127](#)].
- [28] **LHCb** Collaboration, M. Santimaria, *LHC Seminar “New results on theoretically clean observables in rare B-meson decays from LHCb”, 23 March, 2021, .*
- [29] N. G. Deshpande and X.-G. He, *Consequences of R-parity violating interactions for anomalies in $\bar{B} \rightarrow D^{(*)} \tau \bar{\nu}$ and $b \rightarrow s \mu^+ \mu^-$* , *Eur. Phys. J.* **C77** (2017), no. 2 134, [[arXiv:1608.04817](#)].
- [30] D. Das, C. Hati, G. Kumar, and N. Mahajan, *Scrutinizing R-parity violating interactions in light of $R_{K^{(*)}}$ data*, *Phys. Rev.* **D96** (2017), no. 9 095033, [[arXiv:1705.09188](#)].
- [31] K. Earl and T. Grégoire, *Contributions to $b \rightarrow s \ell \ell$ Anomalies from R-Parity Violating Interactions*, *JHEP* **08** (2018) 201, [[arXiv:1806.01343](#)].
- [32] Q.-Y. Hu and L.-L. Huang, *Explaining $b \rightarrow s \ell^+ \ell^-$ data by sneutrinos in the R -parity violating MSSM*, *Phys. Rev. D* **101** (2020), no. 3 035030, [[arXiv:1912.03676](#)].
- [33] Q.-Y. Hu, Y.-D. Yang, and M.-D. Zheng, *Revisiting the B-physics anomalies in R-parity violating MSSM*, *Eur. Phys. J. C* **80** (2020), no. 5 365, [[arXiv:2002.09875](#)].
- [34] W. Altmannshofer, P. B. Dev, A. Soni, and Y. Sui, *Addressing $R_{D^{(*)}}$, $R_{K^{(*)}}$, muon $g - 2$ and ANITA anomalies in a minimal R-parity violating supersymmetric framework*, *Phys. Rev. D* **102** (2020), no. 1 015031, [[arXiv:2002.12910](#)].
- [35] S. Khalil, *Explaining the R_K and R_{K^*} Anomalies With Right-handed Sneutrino*, *J. Phys. G* **45** (2018), no. 12 125004, [[arXiv:1706.07337](#)].
- [36] L. Delle Rose, S. Khalil, S. J. D. King, and S. Moretti, *R_K and R_{K^*} in an Aligned 2HDM with Right-Handed Neutrinos*, *Phys. Rev. D* **101** (2020), no. 11 115009, [[arXiv:1903.11146](#)].
- [37] P. Minkowski, *$\mu \rightarrow e \gamma$ at a Rate of One Out of 10^9 Muon Decays?*, *Phys. Lett. B* **67** (1977) 421–428.

- [38] O. Sawada and A. Sugamoto, eds., *Proceedings: Workshop on the Unified Theories and the Baryon Number in the Universe: Tsukuba, Japan, February 13-14, 1979*, (Tsukuba, Japan), Natl.Lab.High Energy Phys., 1979.
- [39] M. Gell-Mann, P. Ramond, and R. Slansky, *Complex Spinors and Unified Theories*, *Conf. Proc. C* **790927** (1979) 315–321, [[arXiv:1306.4669](#)].
- [40] R. N. Mohapatra and G. Senjanovic, *Neutrino Mass and Spontaneous Parity Nonconservation*, *Phys. Rev. Lett.* **44** (1980) 912.
- [41] J. Schechter and J. W. F. Valle, *Neutrino Masses in $SU(2) \times U(1)$ Theories*, *Phys. Rev. D* **22** (1980) 2227.
- [42] J. Schechter and J. W. F. Valle, *Neutrino Decay and Spontaneous Violation of Lepton Number*, *Phys. Rev. D* **25** (1982) 774.
- [43] G. Lazarides, Q. Shafi, and C. Wetterich, *Proton Lifetime and Fermion Masses in an $SO(10)$ Model*, *Nucl. Phys. B* **181** (1981) 287–300.
- [44] I. Esteban, M. Gonzalez-Garcia, M. Maltoni, T. Schwetz, and A. Zhou, *The fate of hints: updated global analysis of three-flavor neutrino oscillations*, *JHEP* **09** (2020) 178, [[arXiv:2007.14792](#)].
- [45] R. N. Mohapatra, *Mechanism for Understanding Small Neutrino Mass in Superstring Theories*, *Phys. Rev. Lett.* **56** (1986) 561–563.
- [46] R. N. Mohapatra and J. W. F. Valle, *Neutrino Mass and Baryon Number Nonconservation in Superstring Models*, *Phys. Rev. D* **34** (1986) 1642.
- [47] V. De Romeri, K. M. Patel, and J. W. Valle, *Inverse seesaw mechanism with compact supersymmetry: Enhanced naturalness and light superpartners*, *Phys. Rev. D* **98** (2018), no. 7 075014, [[arXiv:1808.01453](#)].
- [48] J. Cao, J. Lian, L. Meng, Y. Yue, and P. Zhu, *Anomalous muon magnetic moment in the inverse seesaw extended next-to-minimal supersymmetric standard model*, *Phys. Rev. D* **101** (2020), no. 9 095009, [[arXiv:1912.10225](#)].
- [49] J. Fidalgo and C. Munoz, *The $\mu\nu$ SSM with an Extra $U(1)$* , *JHEP* **04** (2012) 090, [[arXiv:1111.2836](#)].

- [50] **HFLAV** Collaboration, Y. S. Amhis et al., *Averages of b -hadron, c -hadron, and τ -lepton properties as of 2018*, *Eur. Phys. J. C* **81** (2021), no. 3 226, [arXiv:1909.12524].
- [51] **BaBar** Collaboration, J. P. Lees et al., *Evidence for an excess of $\bar{B} \rightarrow D^{(*)}\tau^-\bar{\nu}_\tau$ decays*, *Phys. Rev. Lett.* **109** (2012) 101802, [arXiv:1205.5442].
- [52] **BaBar** Collaboration, J. P. Lees et al., *Measurement of an Excess of $\bar{B} \rightarrow D^{(*)}\tau^-\bar{\nu}_\tau$ Decays and Implications for Charged Higgs Bosons*, *Phys. Rev.* **D88** (2013), no. 7 072012, [arXiv:1303.0571].
- [53] **Belle** Collaboration, M. Huschle et al., *Measurement of the branching ratio of $\bar{B} \rightarrow D^{(*)}\tau^-\bar{\nu}_\tau$ relative to $\bar{B} \rightarrow D^{(*)}\ell^-\bar{\nu}_\ell$ decays with hadronic tagging at Belle*, *Phys. Rev.* **D92** (2015), no. 7 072014, [arXiv:1507.03233].
- [54] **Belle** Collaboration, S. Hirose et al., *Measurement of the τ lepton polarization and $R(D^*)$ in the decay $\bar{B} \rightarrow D^*\tau^-\bar{\nu}_\tau$* , *Phys. Rev. Lett.* **118** (2017), no. 21 211801, [arXiv:1612.00529].
- [55] **Belle** Collaboration, S. Hirose et al., *Measurement of the τ lepton polarization and $R(D^*)$ in the decay $\bar{B} \rightarrow D^*\tau^-\bar{\nu}_\tau$ with one-prong hadronic τ decays at Belle*, *Phys. Rev.* **D97** (2018), no. 1 012004, [arXiv:1709.00129].
- [56] **Belle** Collaboration, G. Caria et al., *Measurement of $\mathcal{R}(D)$ and $\mathcal{R}(D^*)$ with a semileptonic tagging method*, *Phys. Rev. Lett.* **124** (2020), no. 16 161803, [arXiv:1910.05864].
- [57] **LHCb** Collaboration, R. Aaij et al., *Measurement of the ratio of branching fractions $\mathcal{B}(\bar{B}^0 \rightarrow D^{*+}\tau^-\bar{\nu}_\tau)/\mathcal{B}(\bar{B}^0 \rightarrow D^{*+}\mu^-\bar{\nu}_\mu)$* , *Phys. Rev. Lett.* **115** (2015), no. 11 111803, [arXiv:1506.08614]. [Erratum: *Phys. Rev. Lett.* 115, no. 15, 159901 (2015)].
- [58] **LHCb** Collaboration, R. Aaij et al., *Measurement of the ratio of the $B^0 \rightarrow D^{*-}\tau^+\nu_\tau$ and $B^0 \rightarrow D^{*-}\mu^+\nu_\mu$ branching fractions using three-prong τ -lepton decays*, *Phys. Rev. Lett.* **120** (2018), no. 17 171802, [arXiv:1708.08856].
- [59] **LHCb** Collaboration, R. Aaij et al., *Test of Lepton Flavor Universality by the measurement of the $B^0 \rightarrow D^{*-}\tau^+\nu_\tau$ branching fraction using three-prong τ decays*, *Phys. Rev.* **D97** (2018), no. 7 072013, [arXiv:1711.02505].

- [60] D. Bigi and P. Gambino, *Revisiting $B \rightarrow D\ell\nu$* , *Phys. Rev.* **D94** (2016), no. 9 094008, [[arXiv:1606.08030](#)].
- [61] F. U. Bernlochner, Z. Ligeti, M. Papucci, and D. J. Robinson, *Combined analysis of semileptonic B decays to D and D^* : $R(D^{(*)})$, $|V_{cb}|$, and new physics*, *Phys. Rev.* **D95** (2017), no. 11 115008, [[arXiv:1703.05330](#)]. [erratum: *Phys. Rev.* **D97**, no. 5, 059902 (2018)].
- [62] D. Bigi, P. Gambino, and S. Schacht, *$R(D^*)$, $|V_{cb}|$, and the Heavy Quark Symmetry relations between form factors*, *JHEP* **11** (2017) 061, [[arXiv:1707.09509](#)].
- [63] S. Jaiswal, S. Nandi, and S. K. Patra, *Extraction of $|V_{cb}|$ from $B \rightarrow D^{(*)}\ell\nu_\ell$ and the Standard Model predictions of $R(D^{(*)})$* , *JHEP* **12** (2017) 060, [[arXiv:1707.09977](#)].
- [64] K. Hara, *$R(D)$ and $R(D^*)$ at Belle*, *PoS* **377** (2020) 041.
- [65] **Muon g-2** Collaboration, B. Abi et al., *Measurement of the Positive Muon Anomalous Magnetic Moment to 0.46 ppm*, *Phys. Rev. Lett.* **126** (4, 2021) 2021, [[arXiv:2104.03281](#)].
- [66] **Muon g-2** Collaboration, T. Albahri et al., *Measurement of the anomalous precession frequency of the muon in the Fermilab Muon g-2 experiment*, *Phys. Rev. D* **103** (2021) 072002, [[arXiv:2104.03247](#)].
- [67] **Muon g-2** Collaboration, T. Albahri et al., *Magnetic Field Measurement and Analysis for the Muon g-2 Experiment at Fermilab*, *Phys. Rev. A* **103** (2021) 042208, [[arXiv:2104.03201](#)].
- [68] T. Aoyama et al., *The anomalous magnetic moment of the muon in the Standard Model*, *Phys. Rept.* **887** (2020) 1–166, [[arXiv:2006.04822](#)].
- [69] S. Borsanyi et al., *Leading hadronic contribution to the muon 2 magnetic moment from lattice QCD*, [arXiv:2002.12347](#).
- [70] G. Colangelo, M. Hoferichter, and P. Stoffer, *Two-pion contribution to hadronic vacuum polarization*, *JHEP* **02** (2019) 006, [[arXiv:1810.00007](#)].
- [71] M. Davier, A. Hoecker, B. Malaescu, and Z. Zhang, *A new evaluation of the hadronic vacuum polarisation contributions to the muon anomalous magnetic moment and to*

- $\alpha(\mathbf{m}_Z^2)$, *Eur. Phys. J. C* **80** (2020), no. 3 241, [arXiv:1908.00921]. [Erratum: *Eur.Phys.J.C* 80, 410 (2020)].
- [72] A. Keshavarzi, D. Nomura, and T. Teubner, $g - 2$ of charged leptons, $\alpha(M_Z^2)$, and the hyperfine splitting of muonium, *Phys. Rev. D* **101** (2020), no. 1 014029, [arXiv:1911.00367].
- [73] M. Hoferichter, B.-L. Hoid, and B. Kubis, *Three-pion contribution to hadronic vacuum polarization*, *JHEP* **08** (2019) 137, [arXiv:1907.01556].
- [74] **Muon g-2** Collaboration, G. W. Bennett et al., *Final Report of the Muon E821 Anomalous Magnetic Moment Measurement at BNL*, *Phys. Rev.* **D73** (2006) 072003, [hep-ex/0602035].
- [75] D. Hanneke, S. F. Hoogerheide, and G. Gabrielse, *Cavity Control of a Single-Electron Quantum Cyclotron: Measuring the Electron Magnetic Moment*, *Phys. Rev. A* **83** (2011) 052122, [arXiv:1009.4831].
- [76] T. Aoyama, T. Kinoshita, and M. Nio, *Revised and Improved Value of the QED Tenth-Order Electron Anomalous Magnetic Moment*, *Phys. Rev. D* **97** (2018), no. 3 036001, [arXiv:1712.06060].
- [77] R. H. Parker, C. Yu, W. Zhong, B. Estey, and H. Müller, *Measurement of the fine-structure constant as a test of the Standard Model*, *Science* **360** (2018) 191, [arXiv:1812.04130].
- [78] L. Morel, Z. Yao, P. Cladé, and S. Guellati-Khélifa, *Determination of the fine-structure constant with an accuracy of 81 parts per trillion*, *Nature* **588** (2020), no. 7836 61–65.
- [79] A. Gérardin, *The anomalous magnetic moment of the muon: status of Lattice QCD calculations*, *Eur. Phys. J. A* **57** (2021), no. 4 116, [arXiv:2012.03931].
- [80] J. Hisano and K. Tobe, *Neutrino masses, muon $g-2$, and lepton flavor violation in the supersymmetric seesaw model*, *Phys. Lett. B* **510** (2001) 197–204, [hep-ph/0102315].
- [81] J. E. Kim, B. Kyae, and H. M. Lee, *Effective supersymmetric theory and $(g-2)$ (muon with R -parity violation*, *Phys. Lett. B* **520** (2001) 298–306, [hep-ph/0103054].

- [82] S. P. Martin and J. D. Wells, *Muon Anomalous Magnetic Dipole Moment in Supersymmetric Theories*, *Phys. Rev. D* **64** (2001) 035003, [[hep-ph/0103067](#)].
- [83] D. Stockinger, *The Muon Magnetic Moment and Supersymmetry*, *J. Phys. G* **34** (2007) R45–R92, [[hep-ph/0609168](#)].
- [84] A. S. Belyaev, J. E. Camargo-Molina, S. F. King, D. J. Miller, A. P. Morais, and P. B. Schaefer, *A to Z of the Muon Anomalous Magnetic Moment in the MSSM with Pati-Salam at the GUT scale*, *JHEP* **06** (2016) 142, [[arXiv:1605.02072](#)].
- [85] A. Choudhury, L. Darmé, L. Roszkowski, E. M. Sessolo, and S. Trojanowski, *Muon $g - 2$ and related phenomenology in constrained vector-like extensions of the MSSM*, *JHEP* **05** (2017) 072, [[arXiv:1701.08778](#)].
- [86] A. Choudhury, S. Rao, and L. Roszkowski, *Impact of LHC data on muon $g - 2$ solutions in a vectorlike extension of the constrained MSSM*, *Phys. Rev. D* **96** (2017), no. 7 075046, [[arXiv:1708.05675](#)].
- [87] W. Kotlarski, D. Stöckinger, and H. Stöckinger-Kim, *Low-energy lepton physics in the MRSSM: $(g - 2)_\mu$, $\mu \rightarrow e\gamma$ and $\mu \rightarrow e$ conversion*, *JHEP* **08** (2019) 082, [[arXiv:1902.06650](#)].
- [88] M. Badziak and K. Sakurai, *Explanation of electron and muon $g - 2$ anomalies in the MSSM*, *JHEP* **10** (2019) 024, [[arXiv:1908.03607](#)].
- [89] E. Kpatcha, I. n. Lara, D. E. López-Fogliani, C. Muñoz, and N. Nagata, *Explaining muon $g - 2$ data in the $\mu\nu$ SSM*, *Eur. Phys. J. C* **81** (2021), no. 2 154, [[arXiv:1912.04163](#)].
- [90] S. Heinemeyer, E. Kpatcha, I. n. Lara, D. E. López-Fogliani, C. Muñoz, and N. Nagata, *The new $(g - 2)_\mu$ result and the $\mu\nu$ SSM*, [arXiv:2104.03294](#).
- [91] R. Nagai and N. Yokozaki, *Lepton flavor violations in SUSY models for muon $g - 2$ with right-handed neutrinos*, *JHEP* **01** (2021) 099, [[arXiv:2007.00943](#)].
- [92] J.-L. Yang, T.-F. Feng, and H.-B. Zhang, *Electron and muon $(g - 2)$ in the B-LSSM*, *J. Phys. G* **47** (2020), no. 5 055004, [[arXiv:2003.09781](#)].

- [93] C. Han, M. L. López-Ibañez, A. Melis, O. Vives, L. Wu, and J. M. Yang, *LFV and $(g-2)$ in non-universal SUSY models with light higgsinos*, *JHEP* **05** (2020) 102, [[arXiv:2003.06187](#)].
- [94] J. Cao, Y. He, J. Lian, D. Zhang, and P. Zhu, *Electron and Muon Anomalous Magnetic Moments in the Inverse Seesaw Extended NMSSM*, [arXiv:2102.11355](#).
- [95] J. Cao, J. Lian, Y. Pan, D. Zhang, and P. Zhu, *Improved $(g-2)_\mu$ Measurement and Singlino dark matter in the general NMSSM*, [arXiv:2104.03284](#).
- [96] H.-B. Zhang, C.-X. Liu, J.-L. Yang, and T.-F. Feng, *Muon anomalous magnetic dipole moment in the $\mu\nu$ SSM*, [arXiv:2104.03489](#).
- [97] M. Endo, K. Hamaguchi, S. Iwamoto, and T. Kitahara, *Supersymmetric Interpretation of the Muon $g-2$ Anomaly*, [arXiv:2104.03217](#).
- [98] W. Ahmed, I. Khan, J. Li, T. Li, S. Raza, and W. Zhang, *The Natural Explanation of the Muon Anomalous Magnetic Moment via the Electroweak Supersymmetry from the GmSUGRA in the MSSM*, [arXiv:2104.03491](#).
- [99] S. Baum, M. Carena, N. R. Shah, and C. E. M. Wagner, *The Tiny $(g-2)$ Muon Wobble from Small- μ Supersymmetry*, [arXiv:2104.03302](#).
- [100] M. Abdughani, Y.-Z. Fan, L. Feng, Y.-L. Sming Tsai, L. Wu, and Q. Yuan, *A common origin of muon $g-2$ anomaly, Galaxy Center GeV excess and AMS-02 anti-proton excess in the NMSSM*, [arXiv:2104.03274](#).
- [101] M. Ibe, S. Kobayashi, Y. Nakayama, and S. Shirai, *Muon $g-2$ in Gauge Mediation without SUSY CP Problem*, [arXiv:2104.03289](#).
- [102] M. Van Beekveld, W. Beenakker, M. Schutten, and J. De Wit, *Dark matter, fine-tuning and $(g-2)_\mu$ in the pMSSM*, [arXiv:2104.03245](#).
- [103] P. Cox, C. Han, and T. T. Yanagida, *Muon $g-2$ and Co-annihilating Dark Matter in the MSSM*, [arXiv:2104.03290](#).
- [104] C. Han, *Muon $g-2$ and CP violation in MSSM*, [arXiv:2104.03292](#).

- [105] Y. Gu, N. Liu, L. Su, and D. Wang, *Heavy Bino and Slepton for Muon $g-2$ Anomaly*, [arXiv:2104.03239](#).
- [106] F. Wang, L. Wu, Y. Xiao, J. M. Yang, and Y. Zhang, *GUT-scale constrained SUSY in light of E989 muon $g-2$ measurement*, [arXiv:2104.03262](#).
- [107] A. Aboubrahim, M. Klasen, and P. Nath, *What Fermilab $(g-2)_\mu$ experiment tells us about discovering SUSY at HL-LHC and HE-LHC*, [arXiv:2104.03839](#).
- [108] J.-L. Yang, H.-B. Zhang, C.-X. Liu, X.-X. Dong, and T.-F. Feng, *Muon $(g-2)$ in the B -LSSM*, [arXiv:2104.03542](#).
- [109] W. Altmannshofer, S. A. Gadam, S. Gori, and N. Hamer, *Explaining $(g-2)_\mu$ with Multi-TeV S sleptons*, [arXiv:2104.08293](#).
- [110] J. Rosiek, *Complete Set of Feynman Rules for the Minimal Supersymmetric Extension of the Standard Model*, *Phys. Rev. D* **41** (1990) 3464.
- [111] J. Rosiek, *Complete set of Feynman rules for the MSSM: Erratum*, [hep-ph/9511250](#).
- [112] **CDF** Collaboration, T. Aaltonen et al., *Search for R -parity Violating Decays of τ Sneutrinos to $e\mu$, $\mu\tau$, and $e\tau$ Pairs in $p\bar{p}$ Collisions at $\sqrt{s} = 1.96$ TeV*, *Phys. Rev. Lett.* **105** (2010) 191801, [[arXiv:1004.3042](#)].
- [113] **D0** Collaboration, V. M. Abazov et al., *Search for sneutrino Production in $e\mu$ Final States in 5.3 fb^{-1} of $p\bar{p}$ Collisions at $\sqrt{s} = 1.96$ TeV*, *Phys. Rev. Lett.* **105** (2010) 191802, [[arXiv:1007.4835](#)].
- [114] **ATLAS** Collaboration, G. Aad et al., *Search for a Heavy Neutral Particle Decaying to $e\mu$, $e\tau$, or $\mu\tau$ in pp Collisions at $\sqrt{s} = 8$ TeV with the ATLAS Detector*, *Phys. Rev. Lett.* **115** (2015), no. 3 031801, [[arXiv:1503.04430](#)].
- [115] **CMS** Collaboration, V. Khachatryan et al., *Search for lepton flavour violating decays of heavy resonances and quantum black holes to an $e\mu$ pair in proton-proton collisions at $\sqrt{s} = 8$ TeV*, *Eur. Phys. J.* **C76** (2016), no. 6 317, [[arXiv:1604.05239](#)].
- [116] M. Hirsch, M. A. Diaz, W. Porod, J. C. Romao, and J. W. F. Valle, *Neutrino masses and mixings from supersymmetry with bilinear R parity violation: A Theory for solar*

- and atmospheric neutrino oscillations, *Phys. Rev. D* **62** (2000) 113008, [hep-ph/0004115]. [Erratum: Phys.Rev.D 65, 119901 (2002)].
- [117] I. Esteban, M. Gonzalez-Garcia, A. Hernandez-Cabezudo, M. Maltoni, and T. Schwetz, *Global analysis of three-flavour neutrino oscillations: synergies and tensions in the determination of θ_{23} , δ_{CP} , and the mass ordering*, *JHEP* **01** (2019) 106, [arXiv:1811.05487].
- [118] P. Bhupal Dev, S. Mondal, B. Mukhopadhyaya, and S. Roy, *Phenomenology of Light Sneutrino Dark Matter in cMSSM/mSUGRA with Inverse Seesaw*, *JHEP* **09** (2012) 110, [arXiv:1207.6542].
- [119] J. Chang, K. Cheung, H. Ishida, C.-T. Lu, M. Spinrath, and Y.-L. S. Tsai, *A supersymmetric electroweak scale seesaw model*, *JHEP* **10** (2017) 039, [arXiv:1707.04374].
- [120] T. Moroi, *The Muon anomalous magnetic dipole moment in the minimal supersymmetric standard model*, *Phys. Rev. D* **53** (1996) 6565–6575, [hep-ph/9512396]. [Erratum: Phys.Rev.D 56, 4424 (1997)].
- [121] M. Misiak et al., *Updated NNLO QCD predictions for the weak radiative B-meson decays*, *Phys. Rev. Lett.* **114** (2015), no. 22 221801, [arXiv:1503.01789].
- [122] **HFLAV** Collaboration, Y. Amhis et al., *Averages of b-hadron, c-hadron, and τ -lepton properties as of summer 2016*, *Eur. Phys. J.* **C77** (2017), no. 12 895, [arXiv:1612.07233].
- [123] **LHCb** Collaboration, R. Aaij et al., *Precise determination of the B_s^0 - \overline{B}_s^0 oscillation frequency*, arXiv:2104.04421.
- [124] L. Di Luzio, M. Kirk, A. Lenz, and T. Rauh, *ΔM_s theory precision confronts flavour anomalies*, *JHEP* **12** (2019) 009, [arXiv:1909.11087].
- [125] A. Abada, M. E. Krauss, W. Porod, F. Staub, A. Vicente, and C. Weiland, *Lepton flavor violation in low-scale seesaw models: SUSY and non-SUSY contributions*, *JHEP* **11** (2014) 048, [arXiv:1408.0138].

- [126] J. S. Alvarado and R. Martinez, *PMNS matrix in a non-universal $U(1)_X$ extension to the MSSM with one massless neutrino*, `arXiv:2007.14519`.
- [127] **ATLAS** Collaboration, M. Aaboud et al., *Search for B - L R -parity-violating top squarks in $\sqrt{s} = 13$ TeV pp collisions with the ATLAS experiment*, *Phys. Rev. D* **97** (2018), no. 3 032003, [`arXiv:1710.05544`].
- [128] **ATLAS** Collaboration, C. Sandoval, *Searches for supersymmetry in resonance production, R -parity violating signatures and events with long-lived particles with the ATLAS detector*, *PoS DIS2018* (2018) 081.